Biogeosciences Discuss., 8, 5451–5503, 2011
www.biogeosciences-discuss.net/8/5451/2011/
doi:10.5194/bgd-8-5451-2011

Biogeosciences Discussions

Spatial and temporal CO_2 exchanges measured by Eddy Correlation over a temperate intertidal flat and their relationships to net ecosystem production

P. Polsenaere[1], E. Lamaud[2], V. Lafon[1], J.-M. Bonnefond[2], P. Bretel[1], B. Delille[1,3], J. Deborde[4], D. Loustau[2], and G. Abril[1,5]

[1]Laboratoire Environnements et Paléoenvironnements OCéanique (EPOC), UMR5805, CNRS – Université Bordeaux 1, Avenue des Facultés, 33405 Talence Cedex, France
[2]Laboratoire Ecologie fonctionnelle et PHYSique de l'Environement (EPHYSE), INRA, Centre de Bordeaux-Aquitaine, 71 Avenue Edouard Bourlaux, 33883 Villenave d'Ornon Cedex, France
[3]Unité Océanographie Chimique, Département d'Astrophysique, Géophysique et Océanographie, Université de Liège, 17 Allée du 6 août (Bât. B5), 4000 Liège, Belgium

[4]Institut de Recherche pour le Développement (IRD), 101 Promenade Roger Laroque-Anse Vata BPA5 98848 Nouméa, Nouvelle-Calédonie, France
[5]Institut de Recherche pour le Développement (IRD), Laboratorio de Potamologia Amazônica, LAPA, Universidad Federal do Amazonas, Manaus, Brazil

Received: 23 May 2011 – Accepted: 26 May 2011 – Published: 6 June 2011

Correspondence to: P. Polsenaere (p.polsenaere@epoc.u-bordeaux1.fr)

Published by Copernicus Publications on behalf of the European Geosciences Union.

Abstract

Measurements of carbon dioxide fluxes were performed over a temperate intertidal mudflat in southwestern France using the micrometeorological Eddy Correlation (EC) technique. EC measurements were carried out in two contrasting sites of the Arcachon lagoon during four periods and in three different seasons (autumn 2007, summer 2008, autumn 2008 and spring 2009). In this paper, spatial and temporal variations in vertical CO_2 exchanges at the diurnal, tidal and seasonal scales are presented and discussed. In addition, satellite images of the tidal flat at low tide were used to link the net ecosystem exchange (NEE) with the occupation of the mudflat by primary producers, particularly by *Zostera noltii* meadows. CO_2 fluxes during the four deployments showed important spatial and temporal variations, with the lagoon rapidly shifting from a sink to a source of CO_2. CO_2 fluxes showed generally low negative (influx) and positive (efflux) values and ranged from -13 to $19\,\mu mol\,m^{-2}\,s^{-1}$ at maximum. Low tide and daytime conditions were always characterised by an uptake of atmospheric CO_2. In contrast, during immersion and during low tide at night, CO_2 fluxes where positive, negative or close to zero, depending on the season and the site. During the autumn of 2007, at the innermost station with a patchy *Zostera noltii* bed (cover of 22 ± 14 % in the wind direction of measurements), CO_2 influx was $-1.7 \pm 1.7\,\mu mol\,m^{-2}\,s^{-1}$ at low tide during the day, and the efflux was $2.7 \pm 3.7\,\mu mol\,m^{-2}\,s^{-1}$ at low tide during the night. A gross primary production (GPP) of $4.4\,\mu mol\,m^{-2}\,s^{-1}$ during emersion could be attributed mostly to microphytobenthic communities. During immersion, the water was a source of CO_2 to the atmosphere, suggesting strong heterotrophy or resuspension of microphytobenthic cells. During the summer and autumn of 2008, at the central station with a dense eelgrass bed (92 ± 10 %), CO_2 uptakes at low tide during the day were -1.5 ± 1.2 and $-0.9 \pm 1.7\,\mu mol\,m^{-2}\,s^{-1}$, respectively. Nighttime effluxes of CO_2 were 1.0 ± 0.9 and $0.2 \pm 1.1\,\mu mol\,m^{-2}\,s^{-1}$ in summer and autumn, respectively, resulting in a GPP during emersion of 2.5 and $1.1\,\mu mol\,m^{-2}\,s^{-1}$, respectively, attributed primarily to the seagrass community. At the same station in April 2009, before *Zostera noltii* started to grow,

BGD
8, 5451–5503, 2011

the CO_2 uptake at low tide during the day was the highest ($-2.7 \pm 2.0\,\mu mol\,m^{-2}\,s^{-1}$) and could be attributed to microphytobenthos dominance on NEP in this case. NEE versus PAR relationships for data ranked by wind directions were generally negative where and when *Zostera noltii* was dominant and positive when this community was minor. The latter relationship suggests important processes of photo-acclimatisation by the microphytobenthos, such as migration through the sediment. Influxes of CO_2 were also observed during immersion at the central station in spring and early autumn and were apparently related to phytoplankton blooms occurring at the mouth of the lagoon, followed by the advection of CO_2-depleted water with the tide. Although winter data would be necessary to determine a precise CO_2 budget for the lagoon, our results suggest that tidal flat ecosystems are a modest contributor to the CO_2 budget of the coastal ocean.

1 Introduction

The coastal zone is defined as the ocean area on the continental shelf with a depth of less than 200 m, including all estuarine areas to the upstream limit of tidal influence. The coastal zone receives considerable amounts of nutrients and organic matter from the land, exchanges matter and energy with the open ocean (Borges, 2005) and thus constitutes one of the most biogeochemically active areas of the biosphere (Gattuso et al., 1998; Borges et al., 2005). In the coastal ocean, shallow depth favours light penetration in a large part of the water column and allows for a strong coupling between pelagic and benthic processes. These characteristics make the coastal zone very active in terms of CO_2 exchange, with atmosphere, benthic and pelagic primary production and respiration (Gazeau et al., 2004; Borges et al., 2006). The coastal zone covers approximately 7 % of the surface of the global ocean; despite its relatively modest surface area, this zone accounts for 14–30 % of all oceanic primary production, 80 % of organic matter burial and 90 % of sedimentary mineralisation (Mantoura et al., 1991; Pernetta and Milliman, 1995). In addition, continental shelves act as a net sink

BGD
8, 5451–5503, 2011

of CO_2 of $-0.21 \pm 0.36\,Pg\,C\,yr^{-1}$ – i.e., 15 % of the open ocean sink – whereas nearshore estuarine environments emit $+0.27 \pm 0.23\,Pg\,C\,yr^{-1}$ to the atmosphere (Laruelle et al., 2010). This active but heterogeneous region of the ocean has recently begun to be taken into account in global carbon budgeting efforts (Frankignoulle et al., 1998; Borges, 2005).

The ability of an ecosystem to consume CO_2 and produce organic matter is governed to a large extent by its net ecosystem production (NEP), defined either as the rate of net organic carbon burial and export or as the difference between ecosystem-level gross primary production (GPP) and community respiration (CR) (Smith and Hollibaugh, 1993; Gattuso et al., 1998). GPP represents the C fixation by autotrophic organisms, and CR represents the respiration of all organisms, both autotrophic and heterotrophic. Both GPP and CR are summed per unit ground or water area over time (Chapin et al., 2006). Autotrophic ecosystems have GPP greater than their CR and are net producers of organic C that can be accumulated in the system or exported outside of the system. Heterotrophic ecosystems have GPP lower than their CR and are net consumers of organic C supplied by an external source (Odum, 1956). GPP and CR are processes that also consume and release, on a short timescale, inorganic C in an ecosystem. In a terrestrial system, GPP directly consumes atmospheric CO_2, and CR releases CO_2 directly to the atmosphere. Thus, the net ecosystem exchange (NEE), defined as the net vertical CO_2 exchange between the ecosystem and the atmosphere, is generally approximated by NEP in many terrestrial ecosystems over short timescales (Baldocchi, 2003). In contrast, in aquatic systems, GPP consumes dissolved inorganic carbon and reduces the concentration of CO_2 in the water. This reduction of CO_2 generates a diffusion gradient that causes CO_2 to enter the water from the atmosphere (Chapin et al., 2006). CR in aquatic systems releases CO_2 to the water, where it dissociates into bicarbonate and carbonate ions, generating a water-air CO_2 gradient that tends to emit CO_2 to the atmosphere. Because water-air diffusion is a slow process in comparison with GPP and CR and also compared to lateral water movements, NEE and NEP can be very different over short timescales in aquatic systems (Gattuso et al.,

BGD
8, 5451–5503, 2011

1998; Borges et al., 2006). For instance, a system that receives large amounts of CO_2-saturated water can be autotrophic but also a source of atmospheric CO_2. In addition, a system that receives large amounts of allochthonous organic matter can be heterotrophic but serve as a sink of atmospheric CO_2 if waters are strongly stratified and if the surface layer in contact with the atmosphere becomes net autotrophic. Finally, in aquatic systems, carbonate precipitation and dissolution are additional processes that affect CO_2 concentration: dissolution raises it, whereas precipitation decreases it. For instance, a significant release of CO_2 to waters as a result of carbonate precipitation by invasive benthic macrofauna has been reported in San Francisco Bay (Chauvaud et al., 2003). Inversely, a significant reduction of CO_2 degassing resulting from carbonate dissolution has been reported in a turbid, eutrophic and heterotrophic estuary (Abril et al., 2003).

In the coastal zone, NEP and GPP show important variations both spatially and temporally, depending on a large suite of environmental factors, mainly light and nutrient availability and organic matter loads. Open shelves are net autotrophic and serve as CO_2 sinks (Gazeau et al., 2004; Borges, 2005). Estuaries are generally heterotrophic and are a CO_2 source because of the large inputs of labile organic matter from rivers that fuel CR, while GPP is limited in estuaries by light availability (Smith and Hollibaugh, 1993; Frankignoulle et al., 1998; Borges, 2005). Shallow coastal environments colonised with seagrass meadows are generally net autotrophic, with a GPP estimated at 224.9 ± 11.1 mmol C m^{-2} d^{-1} (Duarte et al., 2010). The intertidal area of the coastal zone also has particular properties with respect to NEP and CO_2 fluxes. First, benthic GPP can be greatly enhanced at low tide because of the increased availability of light and high temperature (Parsons et al., 1984; Hubas et al., 2006). During emersion, benthic NEP is equivalent to NEE. However, during immersion, planktonic and benthic NEP do not necessary correspond to NEE, as a substantial advection of metabolic carbon can occur. Indeed, outwelling of CO_2 supersaturated waters with the tide have been described in salt marsh and mangrove ecosystems (Borges et al., 2003; Wang and Cai, 2004).

BGD
8, 5451–5503, 2011

CO_2 fluxes at the water-air interface can be measured directly using floating chambers (Frankignoulle et al., 1998) or calculated from water partial pressure of CO_2 (pCO_2) measurements and a given gas transfer velocity. However, CO_2 flux computations can be subject to large uncertainties because of the difficulty in accurately assessing the gas transfer velocity (Raymond and Cole, 2001; Vachon et al., 2010). Similarly, the floating chamber method has been suspected to artificially enhance the CO_2 exchange across the air–water interface (Raymond and Cole, 2001). CO_2 fluxes at the air-sediment interface at low tide can be assessed by deploying benthic chambers (Migné et al., 2002), but this method suffers from variability of intertidal sediment habitat resulting from patchiness at all timescales and from spatial patchiness, in particular (Migné et al., 2004). Additionally, surface heating during low tide can also interfere with metabolic processes in tidal flats. Micrometeorological measurements, especially the Eddy Correlation technique (EC), show potential, as CO_2 fluxes across heterogeneous intertidal areas can be obtained with the same technique, at high tide and low tide (Houghton and Woodwell, 1980; Kathilankal et al., 2008; Zemmelink et al., 2009). In addition, the EC method is non-invasive and provides direct and continuous measurements of the net carbon dioxide exchange of a whole ecosystem across a spectrum of time scales from hours to years (Baldocchi, 1988; Aubinet et al., 2000; Baldocchi, 2003). Applying the EC in the coastal zone appears to be a very promising technique, as the method can provide flux data on timescales short enough to resolve the temporal variability induced by the tidal, diurnal and seasonal cycles. However, the method can also have limitations and requires important qualitative and quantitative analyses and corrections because of its physical and theoretical background (Baldocchi et al., 1988; Polsenaere et al., 2011). In intertidal ecosystems, EC measurements present the great advantage of providing precise CO_2 fluxes at the air-water interface during immersion and at the air-sediment interface during emersion. In salt marshes, the EC technique has shown substantial changes in fluxes throughout the tidal cycle (Houghton and Woodwell, 1980; Kathilankal et al., 2008). Likewise, Zemmelink et al. (2009) used the EC technique over the intertidal Wadden Sea mudflat in Europe

BGD
8, 5451–5503, 2011

and observed a CO_2 sink, particularly at low tide and during the day.

On four occasions between 2007 and 2009, we employed an EC system in a lagoon dominated by an intertidal mudflat in south-western France. In a previous paper, (Polsenaere et al., 2011), we presented the methodological aspects of this work and discussed the validity of computed fluxes obtained by EC. In this paper, we present results on the continuous CO_2 fluxes obtained during four different periods over two intertidal areas of the Arcachon lagoon. The main focuses of this paper are (1) to describe and characterise the temporal and spatial variations of CO_2 exchanges occurring in the lagoon during the day and night and during emersion and immersion; (2) to understand the CO_2 flux dynamic in the Arcachon lagoon in relation to the components of NEP (benthic and planktonic GPP and CR) – we focus more specifically on the low tide/day case, during which we could relate CO_2 fluxes to the tidal flat occupation by *Zostera noltii* eelgrass meadows; and (3) to evaluate the CO_2 budget of the lagoon and compare this budget to fluxes reported in other coastal systems.

2 Materials and methods

2.1 Study site

The Arcachon lagoon is a temperate intertidal flat of 174 km^2 on the southwestern Atlantic coast of France (44°40′ N, 01°10′ W). This triangle-shaped bay is enclosed by the coastal plain of Landes Gascony, and communicates with the Atlantic Ocean through a narrow channel 8 km in length (Fig. 1). With a mean depth of 4.6 m, this shallow lagoon presents semi-diurnal tides with amplitudes varying from 0.8 to 4.6 m (Plus et al., 2008). During a tidal cycle, the lagoon exchanges approximately 264×10^6 m^3 and 492×10^6 m^3 of water with the ocean during average neap and spring tides, respectively. The lagoon also receives freshwater, but to a lesser extent, with an annual input of 1.25×10^9 m^3 (1.8×10^6 m^3 at each tidal cycle), of which 8 % is from groundwater, 13 % is from rainfall and 79 % is from rivers and small streams (Rimmelin, 1998). The

BGD
8, 5451–5503, 2011

Leyre River in the southeastern corner of the lagoon represents 73 % of the total freshwater flows (Manaud et al., 1997; De Wit et al., 2005). Water temperatures in the bay vary from 6 °C in winter to 22.5 °C in summer, and water salinity varies from 22 to 35 PSU according to freshwater input variations during the year.

The Arcachon lagoon surface is composed of 57 km^2 of channels, with a maximum depth of 25 m, which drain a large muddy tidal flat of 117 km^2. At two different intertidal sites of the mudflat (Fig. 1), an EC measurement system was deployed on four occasions and during the spring, summer and autumn seasons. A first deployment was made in the inner part of the lagoon at Station 2 (44°42′19.96″ N, 01°04′01.35″ W) in September–October 2007. The three other deployments were carried out at the central station in the lagoon at Station 1 (44°42′59.15″ N, 01°08′36.96″ W) in July 2008, September–October 2008 and in April 2009. During the four experiments, throughout the tidal cycle, the tidal flat was emerged for approximately four hours and immersed for approximately nine hours.

2.2 CO_2 fluxes measured by EC in the Arcachon lagoon

2.2.1 Theory behind the EC technique

The atmosphere contains turbulence (eddies) caused by buoyancy and shear (Aubinet et al., 2000) of upward and downward moving air that transports trace gases such as CO_2 (Baldocchi, 2003). The EC technique allows for the measurement of these turbulent eddies to determine the net flux of any scalar movement vertically across the ecosystem-atmosphere interface.

The mean turbulent flux of the scalar c in the vertical direction (F_c) is expressed as the covariance between the fluctuations in the vertical wind velocity (w) and the scalar density or concentration (ρ_c) (Moncrieff et al., 1997) as

$$F_c = \overline{w' \rho_c'} \quad (1)$$

BGD
8, 5451–5503, 2011

where the overbar represents a temporal average (i.e., 10 min were used in the case of the Arcachon lagoon), and primes denote the instantaneous turbulent fluctuations relative to their temporal average (e.g., $w' = w - \overline{w}$ and $\rho'_c = \rho_c - \overline{\rho_c}$, Reynolds, 1895).

Carbon dioxide fluxes (F_c) can be then defined as

$$F_c = \overline{w'c'} \quad (2)$$

where F_c is expressed in $\mu mol\,m^{-2}\,s^{-1}$, w is expressed in $m\,s^{-1}$ and c (the CO_2 concentration) in $\mu mol\,m^{-3}$. CO_2 fluxes are directed upward when F_c values are positive and downward when corresponding values are negative.

2.2.2 Turbulent flux measurement system in the Arcachon lagoon

Fluxes of CO_2 were measured using an EC system deployed four times in two intertidal flat sites: from 30 September at 11:35 to 3 October 2007 at 08:55 (GMT) at Station 2 (Fig. 1); and from 1 July at 16:40 to 7 July 2008 at 04:00 (GMT), from 25 September at 15:10 to 17 October 2008 at 01:10 (GMT) and from 1 April at 16:30 to 13 April 2009 at 22:50 (GMT) at Station 1, for a total of 4, 7, 20 and 13 days, respectively.

Our EC system (Fig. 2) was fixed to a mast and consisted of a sonic anemometer (model *CSAT3*, Campbell Scientific Inc., Logan, UT) to measure the three wind speed components ($m\,s^{-1}$), as well as the sonic temperature (°C), and an infra-red gas analyser (model *LI-7500*, Licor Inc., Lincoln, NE) that measured CO_2 and H_2O concentrations ($mmol\,m^{-3}$) and atmospheric pressure (kPa). Analogue output signals from these fast-response instruments were sampled and digitised at the rate of 20 Hz. With these two main EC sensors separated by a distance of 0.25 m, a filtered silicon quantum sensor (*SKP215*, Skype Instruments, Llandrindod Wells, UK) was used to measure photosynthetically active radiation (PAR, $\mu mol\,m^{-2}\,s^{-1}$) every minute (Fig. 2b). Additionally, a meteorological transmitter (model *WXT510*, Vaisala Inc., Finland) was set up in September–October 2008 and April 2009. This transmitter provided additional wind speed and direction measurements that could be compared with data from the

BGD
8, 5451–5503, 2011

sonic anemometer and other weather parameters: air temperature, pressure, humidity, and the amount, intensity and duration of rainfall events. The sensors were mounted on a mast inserted in the mud and secured by three wires to keep it vertical and to limit vibrations that could bias EC flux measurements (Fig. 2a). Data were recorded by a central acquisition system (model *CR3000*, Campbell Scientific Inc., Logan, UT) (connected to the sensors with a waterproof cable) located in an anchored inflatable raft and protected by a tide pool. The entire system was powered by rechargeable lead batteries (12 volts, 100 amperes per hour) and replaced every four days.

The equipment used was similar for the four deployments except during September–October 2007, when a different sonic anemometer (model *Windmaster*, Gill Instr., UK) was used, as well as a different sample frequency for both EC sensors, i.e., 10 Hz. Also during this deployment, the PAR was not directly measured at the EC station but at the Cap Ferret meteorological station (44°37′54″ N, 01°14′54″ W). Global radiation ($J\,cm^{-2}$) hourly data were first obtained and then converted to $W\,m^{-2}$ and to $\mu mol\,m^{-2}\,s^{-1}$, assuming a factor of 2 from $W\,m^{-2}$ to $\mu mol\,m^{-2}\,s^{-1}$, to homogenise PAR units between the four deployments. The sensors for the four field setups were mounted at maximum heights (during low tide) of 4.20, 5.50, 7.0 and 5.0 m in September–October 2007, July 2008, September–October 2008 and April 2009, respectively.

2.2.3 Data processing and quality control

Raw data were processed following the Aubinet et al. (2000) methodology developed in the context of the EUROFLUX project for net carbon and water exchanges of forests and modified to be applied to intertidal areas. The first important adaptation of the forest-based methodology to the case of the Arcachon mudflat was to adjust for variations in the relative measurement height with the tidal rhythms, which must be included in EC data computations and corrections. Secondly, fluxes were computed with a shorter averaging period (10 min) than usually used (30 min) to detect the quick transitions from low tide to high tide and vice versa. A detailed description of the data

BGD
8, 5451–5503, 2011

processing used here is given in Polsenaere et al. (2011). To summarise, data were processed using the EdiRe software from the University of Edinburg (Scotland) by applying the following steps: (1) spike removal in anemometer or gas analyser data; (2) unit modifications and statistical operations; (3) coordinating rotation to align coordinate system with the stream lines of the 10 min. averages; (4) linear de-trending of sonic temperature, H_2O and CO_2 channels; (5) determining time lag values for H_2O and CO_2 channels using a cross-correlation procedure; (6) computing mean values, turbulent fluxes and characteristic parameters, e.g., the Monin-Obhukov stability index Z/L; (7) high-frequency corrections via transfer functions based on Kaimal-Moore's co-spectral models (Kaimal et al., 1972; Moore, 1986); and (8) performing a Webb-Pearman-Leuning correction to account for the effects of fluctuations of temperature and water vapour on measured fluctuations in CO_2 and H_2O (Webb et al., 1980).

In parallel to frequency corrections, a cospectral analysis was carried out for each period to quantify the distribution by frequency of the covariance of the raw measured signals. In particular, the power cospectra between the vertical wind velocity and carbon dioxide were computed and analysed as detailed in Polsenaere et al. (2011).

According to data quality control protocols, incorrect processed data must be removed to obtain reliable CO_2 flux measurements. Several factors can lead to bias or errors, i.e., instrument malfunctions, processing/mathematical artefacts, ambient conditions not satisfying the EC methodology (non-stationary periods, convergence, divergence), heavy precipitation – particularly for open-path gas analyser – or a measurement footprint larger than the fetch of interest (Burba and Anderson, 2005). An adapted procedure developed for the Arcachon lagoon study is presented in Polsenaere et al. (2011). Two main statistical tests were used: (1) the steady-state test was applied to pairs of specified signals, particularly to w and c in this study. Standard deviations and covariances of w and c were computed on short time intervals of 1 min, and these values were compared to those computed on the chosen time run of 10 min, following Foken and Wichura (1996). Only data corresponding to a difference lower than 30 % (periods defined as steady-state conditions) were retained. (2) The

BGD
8, 5451–5503, 2011

statistical test was based on the integral turbulence characteristics of wind components and temperature, according to Foken et al. (1991, 1997). The σ_w/u^* and σ_T/T^* ratios of the data signals (where σ is the standard deviation of the specified signals) were computed and compared to their parameterised values according to different ranges of stability (Z/L parameter). Only data matching with a difference of less than 50 % were retained. Using these two statistical tests, the retained EC data for the Arcachon lagoon corresponded to "high-quality data" with a general flag from 1 to 3, according to Foken (2003). In the end, 73 %, 83 %, 83 % and 87 % of CO_2 flux data were retained for the September–October 2007, July 2008, September–October 2008 and April 2009 periods, respectively.

2.3 Eelgrass retrieval from satellite data

The fetch around the mast always ranged between at least 1000 m at Station 1 and 700 m at Station 2 at low tide in all the wind directions (Fig. 1). Thus, we can assume that all measured fluxes were from the intertidal area of interest, the fetch being generally larger than the footprint of the measurements. Indeed, the relative maximum sensor height at low tide was 4.20 m at Station 2 and ranged between 5 and 7 m at Station 1; it is generally accepted that the relative height:fetch ratio must be lower than 1:100 and lower than 1:300 for unstable and stable atmospheric conditions, respectively (Leclerc and Thurtell, 1990; Hsieh et al., 2000). Thus our fetch distances of at least 1000 m and 700 m at Station 2 and 1 respectively fulfill this assumption most of the time for stable conditions and all of the time for unstable conditions, which are more frequent in the lagoon (Polsenaere et al., 2011).

To relate the temporal and spatial variations in the measured for NEE with the distribution of vegetation on the mudflat, satellite images at low tide during the day were analysed. The occupation of the *Zostera noltii* eelgrass meadows was quantified within a circle of 1 km radius centred on the EC mast for both sites. Each circle was then divided into eight sectors corresponding to different wind directions: 0–45°: north-northeast, 45–90°: east-northeast, 90–135°: east-southeast, 135–180°:

BGD
8, 5451–5503, 2011

south-southeast, 180–225°: south-southwest, 225–270°: west-southwest, 270–315°: west-northwest and 315–360°: north-northwest wind directions. Satellite images from SPOT were processed using the methodology based on the normalised vegetation index (Barillé et al., 2010). With the exception of the very low eelgrass densities that can be confused with microphytobenthos, the seagrass meadow surfaces can be assessed and the associated cover density can be derived from these images. This approach has been applied to the retrieval of the meadows at Arcachon. For this purpose, images from the CNES/Kalideos database were used. Georeferenced images were downloaded and calibrated using field reflectance data. Finally, channel surfaces, oyster farms, and salt marshes were masked, before calculating the vegetation index on a pixel basis. The eelgrass position and density were deduced from the 2-D mapped index. A dataset of 36 GPS observations collected during autumn 2009 were compared to a SPOT map derived from an image acquired 8 September 2009. The results show that ground-truthing corroborated the map in approximately 90 % of the cases. This test validates this mapping approach that was applied to the five satellite images used in this study.

In all, we analysed five images corresponding to the lagoon at low tide during the day. The first was recorded on 13 September 2007, precisely matching with the EC deployment carried out in autumn 2007 at Station 2 in the back of the lagoon. The second image, recorded on 17 October 2008, matched the deployment made in autumn 2008 at Station 1 in the centre of the lagoon. The third image, recorded at the same station and at the same season the next year, on 8 September 2009, was solely used to describe the inter-annual change of the seagrass meadow. Finally, no image precisely matched the deployment from spring 2009 at Station 1, with the closest matching image recorded on 24 June 2009. A fifth image, recorded the next year at Station 1 on 14 April 2010, was also analysed. The latter two images provided insights on the possible changes of the meadow during the spring period.

BGD
8, 5451–5503, 2011

3 Results

Because diurnal and tidal rhythms largely controlled the CO_2 fluxes, the following results refer to the four distinct cases generated by these two cycles: emersion around low tide during the day (LT/Day), emersion at night (LT/Night), immersion around high tide during the day (HT/Day) and immersion at night (HT/Night). The dynamics of the NEE in relation to the environmental parameters are described for each EC measurement as presented in Table 1 and Figs. 3, 4, 5 and 6.

3.1 Autumn 2007 at Station 2

Over the four days of measurements in September–October 2007 at Station 2, the Arcachon lagoon acted as a source of CO_2 to the atmosphere, with an average of $0.8 \pm 2.7\,\mu mol\,m^{-2}\,s^{-1}$ and fluxes ranging from -10.0 to $18.6\,\mu mol\,m^{-2}\,s^{-1}$ (Table 2, Fig. 3e). However, at low tide during sunny afternoons with PAR values reaching more than $1000\,\mu mol\,m^{-2}\,s^{-1}$ at midday (Fig. 3a), strong CO_2 uptakes (CO_2 sinks) were systematically observed, as seen on Days 273 and 274, with values close to 6 and $-10\,\mu mol\,m^{-2}\,s^{-1}$, respectively (Fig. 3e). In contrast, during nighttime at low tide, the lagoon emitted large quantities of CO_2 to the atmosphere, acting as a CO_2 source ($2.7 \pm 3.7\,\mu mol\,m^{-2}\,s^{-1}$ on average, Table 1), as measured between Days 273 and 274 and between Days 275 and 276, with values largely above $10\,\mu mol\,m^{-2}\,s^{-1}$ (Fig. 3e). The CO_2 uptake observed at LT/Day 275 was weak, reaching only $2\,\mu mol\,m^{-2}\,s^{-1}$, compared to that observed on preceding days (Fig. 3e); this change corresponded to the occurrence of a mass of relatively hot air (approaching 24°C, Fig. 3b) concomitant with a change in wind direction from the east-southeast (90–135°) to south-southwest (180–225°) (Fig. 3d) sectors and with a higher speed, above $5\,m\,s^{-1}$ (Fig. 3c).

BGD
8, 5451–5503, 2011

3.2 Summer 2008 at Station 1

In July 2008, at Station 1, the Arcachon lagoon showed weaker CO_2 exchanges than in autumn 2007 at Station 2, acting on average as a small source of CO_2 to the atmosphere over the week ($0.1 \pm 1.9\,\mu mol\,m^{-2}\,s^{-1}$), with CO_2 fluxes ranging generally from -5.75 to $2\,\mu mol\,m^{-2}\,s^{-1}$ (Fig. 4e, Table 1). During summer 2008 at LT/Day, high CO_2 uptakes were measured, reaching values of $-5\,\mu mol\,m^{-2}\,s^{-1}$, as observed during Day 187 (Fig. 4e). These CO_2 sinks occurred particularly during sunny days, with PAR values close to $1500\,\mu mol\,m^{-2}\,s^{-1}$ at midday, and were roughly synchronised with low tides (from Days 185 to 188, Fig. 4a). PAR values measured during this season showed variable but intense radiations above $2000\,\mu mol\,m^{-2}\,s^{-1}$ at midday (Days 185 and 186, Fig. 4a). At LT/Night, CO_2 emissions to the atmosphere were measured, with CO_2 flux values generally above $2\,\mu mol\,m^{-2}\,s^{-1}$ (Fig. 4e). At the beginning of the measurement (Days 183 and 184), this classical scheme of CO_2 uptake at LT/Day and CO_2 degassing at LT/Night was perturbed and replaced by a strong CO_2 source to the atmosphere, also at LT/Day, reaching $12\,\mu mol\,m^{-2}\,s^{-1}$ (Fig. 4e). During this event, PAR values were below $500\,\mu mol\,m^{-2}\,s^{-1}$ at midday (Fig. 4a), and a particular mass of air coming from the south-southwest wind sector (180–225°) changed in speed, reaching $8\,m\,s^{-1}$, and in direction (Fig. 4c and d).

3.3 Autumn 2008 at Station 1

Contrary to the previous measurements, in September-October 2008 at Station 1, the Arcachon lagoon was a sink of CO_2 over the twenty days, with an average uptake of $0.2 \pm 1.4\,\mu mol\,m^{-2}\,s^{-1}$ and the CO_2 fluxes ranging generally from -5.0 to $3.0\,\mu mol\,m^{-2}\,s^{-1}$ (Table 1). During this deployment, medium CO_2 sinks were measured at LT/Day, with values generally close to $-5\,\mu mol\,m^{-2}\,s^{-1}$ (i.e., Days 287 and 289), whereas weak CO_2 sources were found at LT/Night below $3\,\mu mol\,m^{-2}\,s^{-1}$ (i.e., Days 286 and 288) (Fig. 5e). The PAR values were typical for the season, with some

BGD
8, 5451–5503, 2011

values close to 1250 µmol m^{-2} s^{-1} being measured at midday during sunny days. The PAR values were slightly higher than those measured during the same season in 2007 at Station 2, probably because of the presence of clouds during the three days of measurement. At Station 1, PAR values observed at midday decreased over the twenty days of measurement, from 1500 µmol m^{-2} s^{-1} to 1300 µmol m^{-2} s^{-1}, i.e., at a rate of −10 µmol m^{-2} s^{-1} each day (Fig. 5a). As noted in the previous measurements, reductions in CO_2 influxes at LT/Day and in CO_2 effluxes at LT/Night with immersion were observed. Indeed, during Day 276, the CO_2 flux shifted in less than one hour from −1.5 µmol m^{-2} s^{-1} at LT to −0.7 µmol m^{-2} s^{-1} with 30 cm of water, whereas the PAR remained high and constant (Fig. 5e). During flood tide on Night 279/280, CO_2 degassing decreased from 1.0 to 0.2 µmol m^{-2} s^{-1} in less than one hour after the tidal flat immersion. Contrary to September–October 2007 at Station 2 and July 2008 at Station 1, CO_2 influxes were measured at HT/Night (−0.3 ± 1.3 µmol m^{-2} s^{-1} on average, Table 1), as found during Night 282/283, with values reaching −7 µmol m^{-2} s^{-1} (Fig. 5e). In addition, a strong CO_2 emission of 14 µmol m^{-2} s^{-1} was observed at LT/Day (Day 279) immediately after a sudden and concomitant increase in air temperature and wind speed (Figs. 5b and c) and a switch in wind direction to the 180–225° sector (Fig. 5d).

3.4 Spring 2009 at Station 1

In April 2009, the strongest CO_2 sink was measured in the Arcachon lagoon, with −2.4 µmol m^{-2} s^{-1} on average and CO_2 fluxes ranging from −13 to 3 µmol m^{-2} s^{-1} over the thirteen days of measurement (Table 1). No clear pattern was observed, in contrast to the previous measurements, with the CO_2 fluxes always negative regardless of the diurnal or the tidal phase (Fig. 6e). Nevertheless, the largest sinks of CO_2 also occurred at LT/Day (i.e., Days 93 and 103), and fluxes were close to zero or positive as soon as night fell, in particular at low tide (i.e., Nights 98/99 and 100/101) (Fig. 6e). At LT/Day during Days 95 and 96, weaker CO_2 influxes corresponded to cold masses of air close to 13 °C with low wind speeds near 1 m s^{-1} and wind directions from the

BGD
8, 5451–5503, 2011

south-southeast (135–180°) (Fig. 6b, c, d and e). In contrast to the three previous measurement periods, when LT/Night cases always corresponded to CO_2 releases to the atmosphere due to benthic respiration, in April 2009, CO_2 fluxes at LT/Night were either null or negative (Table 1 and Fig. 6e). In fact, these negative fluxes occurred during very short periods of LT/Night, at the end (Day 94) or at the beginning (Days 94/95 and 95/96) of the night and immediately after or before immersion (Fig. 6e). In conditions of well-established LT/Night conditions (Days 92, 97, 98, 100 and 101), CO_2 fluxes were null.

3.5 Wind direction, CO_2 fluxes and Zostera noltii cover

Figure 7 presents the occurrence of prevailing winds per sector for each period. Wind directions varied temporally according to the season and also spatially according to the station. In September–October 2007 at Station 2, the prevailing winds blew mostly from the east-southeast and east-northeast, with 60 % and 27 % of occurrence, respectively (Fig. 7a). In autumn 2008 at Station 1, no wind direction clearly prevailed; the north-northeast (0–45°) and south-southeast (135–180°) sectors both accounted for 20 % of the wind, and the 180–315° sector accounted for less than 10 % (Fig. 7b). During July 2008 and April 2009 at Station 1, wind direction also changed often, but consistent prevailing winds occurred from the 225–315° and the 270–360° sectors. Consequently, winds from the west-northwest were mostly observed during both seasons, reaching more than 40 % in summer 2008 and 30 % of occurrence in spring 2008 (Fig. 7c, d).

The analyses of satellite images of the lagoon at LT/Day in relation to the percentage of EC measurements for each period are presented in Table 2. In autumn 2007 at Station 2, seagrass cover was generally low, ranging between 4 % and 51 % from the south-southwest and east-southeast wind sectors, respectively (Table 2). More than 60 % of the CO_2 flux data corresponded to the highest *Zostera noltii* cover (27 % from the east-southeast sector) and the more negative averaged CO_2 flux ($-2.1 \pm 1.4\,\mu mol\,m^{-2}\,s^{-1}$, Table 2). Inversely, more than 20 % of the data matched the lowest seagrass cover (4 % from the south-southwest sector) and one of the least

BGD
8, 5451–5503, 2011

negative averaged CO_2 fluxes ($-0.7 \pm 0.6\,\mu mol\,m^{-2}\,s^{-1}$, Table 2). In summer 2008 at Station 1, where no satellite image was available, almost 50 % of F_c data were measured from the west-northwest sector, with a flux of $-2.0 \pm 1.4\,\mu mol\,m^{-2}\,s^{-1}$ on average (Table 2). In autumn 2008 at the same station, higher *Zostera noltii* covers were measured than during the same season in 2007 at Station 2, with values ranging between 70 % (south–southeast) and 99 % (west-northwest) (Table 2). A total of 21 % and 17 % of flux data (-0.9 ± 1.0 and $-0.7 \pm 1.3\,\mu mol\,m^{-2}\,s^{-1}$ on average) corresponded to covers of 70 % (south–southeast) and 93 % (east–northeast), respectively. The next year, in autumn 2009, exactly the same percentage of *Zostera noltii* cover was observed (92 ± 10 % in average), between 69 and 99 % (Table 2). These results are in particular in accordance with the study of Auby and Labourg (1996), who showed that seagrass generally reaches maximum densities of biomass in summer–autumn in the Arcachon lagoon. In spring 2009 at Station 1, where no images matched precisely with the EC deployment, approximately 30 % of F_c data corresponded to the west-northwest and north-northwest wind sectors, with average fluxes of -3.0 ± 1.5 and $-3.1 \pm 1.2\,\mu mol\,m^{-2}\,s^{-1}$, respectively (Table 2). The analysis of the image recorded on April 2010 (14 April), the year after the EC deployment, showed very low seagrass cover, below 5 %, regardless of wind direction (data not shown). In fact, seagrass leaves only begin to grow in spring, showing rather low above-ground biomass, and the minimum values are observed in winter, with a root system (rhizome) persisting throughout the year (Duarte, 1989; Auby and Labourg, 1996; Vermaat and Verhagen, 1996). The image recorded on 24 June 2009 at Station 1 showed slightly lower seagrass cover than in late summer–autumn (range: 62–97 %) but higher than that measured previously, in early spring 2010. However, this image, obtained two months after the EC deployment carried out in April 2009, may represent the evolution of the meadow over the spring period in terms of ecological processes. The image could then be used to link the CO_2 fluxes and the seagrass cover measured in this period at Station 1. In particular, the more negative CO_2 flux ($-4.5 \pm 2.6\,\mu mol\,m^{-2}\,s^{-1}$, in average) measured in April 2009 corresponded to the highest *Zostera noltii* cover (97 %) observed

BGD
8, 5451–5503, 2011

in June 2009 from the west-southwest sector of wind direction (Table 2). Inversely, the less negative CO_2 fluxes ($-1.0 \pm 1.6\,\mu mol\,m^{-2}\,s^{-1}$, in average) corresponded to the lowest seagrass cover (62 %) from the south–southeast wind sector (Table 2).

4 Discussion

4.1 Spatial and temporal variations of NEE in relation to the NEP of the Arcachon lagoon

4.1.1 Relationship between low tide CO_2 fluxes and the distribution of *Zostera noltii* meadows

Zostera noltii Hornem. is a common intertidal seagrass of the European and African coasts distributed from Norway to Mauritania (Den Hartog, 1970). It constitutes an important and highly productive component of the benthic environment in these near-shore soft-bottom ecosystems (McRoy and McMillan, 1977). In the Arcachon lagoon, *Zostera noltii* beds are particularly extensive, colonising the major part of the intertidal area (60 %, i.e., 70 km^2) between −1.9 m and +0.8 m relative to local Mean Sea Level (Amanieu, 1967).

With regard to satellite images, a significant spatial difference in *Zostera noltii* cover was observed at Stations 2 and 1 during the same season in autumn 2007 and 2008 (Table 2). Even if late summer coincides with maximum in *Zostera noltii* biomass, in September–October 2007 in the inner part of the lagoon, the percentage of occupation by the seagrass was only 22 ± 14 % on average. In contrast, in September–October 2008 in the middle of the lagoon at Station 1, the cover of *Zostera noltii* was much more important, with a mean of 92 ± 10 % (Table 2). This spatial distribution is in strong agreement with the extent of the *Zostera noltii* seagrass beds in 2007 in the lagoon reported by Plus et al. (2010).

BGD
8, 5451–5503, 2011

For the low tide conditions, we assumed that benthic CR was equivalent to NEE at night (Rocha and Goulden, 2008), and benthic NEP was equivalent to NEE averaged over the daytime. GPP at low tide can be calculated as the NEE during the day plus the NEE at night, as presented in Table 3. In autumn 2007 at Station 2 with a low *Zostera noltii* density, a particularly high GPP of 4.4 $\mu mol\,m^{-2}\,s^{-1}$ was calculated, the CR showing the highest value, with $2.7 \pm 3.7\,\mu mol\,m^{-2}\,s^{-1}$, resulting in an NEP of $1.7 \pm 1.7\,\mu mol\,m^{-2}\,s^{-1}$ (Table 3). In contrast, in autumn 2008 at Station 1 with a high *Zostera noltii* density, a slightly low GPP of 1.09 $\mu mol\,m^{-2}\,s^{-1}$ was found, the CR being moderate, equal to $0.2 \pm 1.1\,\mu mol\,m^{-2}\,s^{-1}$, resulting in an NEP of $0.9 \pm 1.7\,\mu mol\,m^{-2}\,s^{-1}$ (Table 3). In parallel, at both stations, rapid changes in CO_2 fluxes (NEP) were observed in relation to wind direction and seagrass cover; the most negative (the highest NEP) and the least negative (the lowest NEP) CO_2 fluxes matched the highest and the lowest seagrass cover, respectively (Table 2). These results indicate that *Zostera noltii* appears to greatly control the NEP (GPP and CR) in autumn at Station 1 where the cover is high, but only partly controls the NEP at Station 2, where the cover is low. In contrast, microphytobenthos communities appear to significantly contribute to the GPP at Station 2 in autumn, where *Zostera noltii* meadow cover is low. The production of these communities in the lagoon is estimated to be between 104 and 114 $g\,C\,m^{-2}\,yr^{-1}$, of the same order as the production of *Zostera noltii* (Auby, 1991). Such high GPP by microphytobenthos at low tide in intertidal mudflats has already been reported by Guarini (1998) in the Marennes-Oléron basin (France), by Migné et al. (2004) in the Bay of Somme (eastern English Channel, France), by Spilmont et al. (2006) in the mudflat of the Seine Estuary (English Channel, France), and by Hubas et al. (2006) in the intertidal bay of Roscoff Aber. In addition, in September–October 2007 at Station 2, the highest CR (LT/Night) is probably accounted for by the intense grazing of meiofauna and macrofauna on microphytobenthos, the latter being easily and rapidly transferred toward superior benthic heterotrophic components in intertidal areas (Middelburg et al., 2000; Spilmont et al., 2006). Our results suggest the occurrence of two superimposed metabolic carbon cycles in the lagoon, functioning at different timescales: a rapid C

BGD
8, 5451–5503, 2011

cycling (high GPP and CR), ensured by microphytobenthic communities at Station 2 (tide or week scales), and a slow C cycle (low GPP and CR), ensured by the seagrass meadows at Station 1 (seasonal scale).

GPP and CR calculations could not be performed for the data obtained in April 2009 (Station 1), as discussed previously; CO_2 fluxes over the mudflat were null or slightly negative at LT/Night and could not be attributed to benthic CR at low tide. In the unvegetated tidal flat of the Wadden Sea at the same season, Zemmelink et al. (2009) reported null and negative CO_2 fluxes with both EC and chamber techniques. Several processes could partly explain these fluxes in the Arcachon mudflat during this season, when the *Zostera noltii* cover was low and is generally dominated by microphytobenthic GPP, as shown by Spilmont et al. (2006) in the Seine Estuary (France). First, microphytobenthic cells can migrate down to deeper layers of the sediment at night as protection against grazing by deposit-feeders (Blanchard et al., 2001); thus, respiration would not release CO_2 to the atmosphere but deeper into the sediments. Second, CO_2 generated by benthic respiration could be almost entirely involved in the dissolution of carbonate shells and not released to the atmosphere, as occurred for instance in a Mediterranean seagrass meadow (*Posidonia oceanica*) in winter (Barrón et al., 2006).

Concerning seasonal variations at Station 1, in July 2008, the values of GPP ($2.5\,\mu mol\,m^{-2}\,s^{-1}$) and CR ($1.0 \pm 0.9\,\mu mol\,m^{-2}\,s^{-1}$) were similar to those obtained in September–October 2008, resulting in an NEP of $1.5 \pm 1.2\,\mu mol\,m^{-2}\,s^{-1}$ (Table 3). This result suggests that at Station 1 during the summer season, the predominance of *Zostera noltii* on the NEP (GPP and CR) was similar to that noticed during the early autumn at the same station. In spring 2009, a stronger NEP ($-2.7 \pm 2.0\,\mu mol\,m^{-2}\,s^{-1}$, Table 2) was measured at LT/Day in comparison to the NEP values measured in summer-autumn 2008. In addition, as in autumn 2007 at Station 2, in April 2009 at Station 1, rapid changes in CO_2 fluxes were measured, with wind direction and *Zostera noltii* cover obtained in June 2009; in particular, the more negative (the strongest NEP) and less negative (the lowest NEP) CO_2 fluxes matched the highest and lowest seagrass cover (Table 2). This finding suggests that *Zostera noltii* partly controls the NEP at

BGD
8, 5451–5503, 2011

Station 1 during the spring season. In contrast, the NEP, and more specifically the GPP, is probably driven by microphytobenthos communities during early spring at Station 1, where *Zostera noltii* cover is still low as its growth period is just starting. During each spring season, the mud sediments of the intertidal area of the Arcachon lagoon are notably the location of strong microphytobenthic biomasses; they produce a brown biofilm above the sediment surface and present an intense photosynthetic activity.

The changes in the relative importance of these two main primary producers at Station 1 throughout the year do not indicate clearly significant differences in the benthic production of the Arcachon lagoon. This result is in opposition to the study of Hubas et al. (2006), who showed in bare sediments in the bay of Morlaix that only one primary producer strongly contributed to community production. In contrast, the present study is in agreement with the study of Ouisse et al. (2010) in the same bay, who observed a changing importance of primary producers (*Zostera noltii*, associated epiphytes and benthic microalgae) over the course of the year, resulting in a relatively constant rate of production at the community scale.

To clarify and complete our analysis about the control of the CO_2 fluxes in the tidal flat at LT/Day, P-I relations ranked by wind direction and *Zostera noltii* cover were analysed (Fig. 8). In September–October 2007 at Station 2, no correlation between NEE and PAR was found. Additionally, in July 2008 at Station 1, no clear patterns were observed, as discussed in Polsenaere et al. (2011). However, when data were classified according to sectors of wind direction, negative NEE vs. PAR linear regressions were found, particularly from the east-southeast wind direction (90–135°) and two others showing a similar shape, from the south-southwest (180–225°) and the west-southwest (225–270°) wind directions (Fig. 8a). Contrasts in *Zostera noltii* densities between the 90–135° and 180–270° sectors in July 2008 at Station 1, could explain the differences observed by the EC technique. In September–October 2008 at the same station, a similar NEE-PAR relation (Fig. 8b) was observed for the west-southwest direction, matching the strongest CO_2 uptake and the most extensive seagrass meadow (Table 2). Such negative correlations have been observed with EC by Morison et al. (2000) for

BGD
8, 5451–5503, 2011

the C_4 aquatic grass *Echinochloa polystachya* of the Amazon and by Kathilankal et al. (2008) for the *Spartina alterniflora* in a salt marsh on the eastern coast of Virginia. Using benthic incubations, Silva et al. (2005) obtained the same results for *Zostera noltii* meadows in the intertidal flats of the Ria Formosa lagoon in Portugal. These negative correlations between NEE and PAR (or positive correlations between CO_2 uptake by the vegetated community and the intensity of available light) suggest an optimal adaptation of the plants to environmental conditions, such as temperature, humidity and light.

In April 2009 at Station 1, negative linear regressions were measured from the west-southwest (225–270°) and north-northwest wind directions (315–360°), matching the highest seagrass cover observed in June 2009 (Fig. 8c and Table 2). Nevertheless, positive relations were also obtained for three continuous wind direction sectors covering 90–135°, which notably matched the lowest *Zostera noltii* cover (Fig. 8d and Table 2). This result is in opposition to other studies carried out in intertidal mudflats, which systematically reported negative correlations between CO_2 fluxes and irradiance (Guarini, 1998; Migné et al., 2004, 2007; Spilmont et al., 2006). During this spring period, microphytobenthic communities, generally diatoms in the majority, are known to dominate benthic GPP in the lagoon, forming dense mats on the mudflat (Auby, personal communication). Even, microphytobenthic cells living as epiphytes on young *Zostera noltii* leaves could represent a significant part of the benthic GPP, especially in winter and early spring, as shown by Ouisse et al. (2010) in an intertidal *Zostera noltii* bed (Western English Channel, France). The lack of correlation between NEE and air temperature for these three wind directions suggest that CR is not stimulated by surface heating. Photoinhibition of photosynthesis may also occur, but this mechanism has been observed primarily in laboratory and rarely in field conditions (Blanchard and Cariou-Le Gall, 1994; Guarini, 2000). Finally, it has been shown that microphytobenthic cells can migrate vertically through the sediments to protect them in response to long periods of light exposure at LT/Day as behavioural process of photo-acclimatisation (Blanchard et al., 2004; Serôdio et al., 2008). In consequence, this last hypothesis may

BGD
8, 5451–5503, 2011

explain the positive NEE-PAR correlations obtained in April 2009. Figure 8e presents the processes implied at this period with negative and positive NEE-PAR slopes associated with the highest and the lowest *Zostera noltii* covers, respectively. These results may confirm the previous concept of the concomitant presence of young *Zostera noltii* leaves together with microphytobenthic epiphytes and microphytobenthic mats on sediments in spring 2009 at Station 1.

4.1.2 Diurnal and tidal changes in NEE during the different seasons

Throughout the diurnal and tidal cycles, variations in NEE were large, with the lagoon often rapidly shifting from source to sink. For instance, at Station 1 in July 2008 on Day 184 and daytime, NEE rapidly dropped from 12.0 $\mu mol\,m^{-2}\,s^{-1}$ at low tide to $-5.0\,\mu mol\,m^{-2}\,s^{-1}$ as soon as the water submerged the flat. Inversely, at night, between Days 187 and 188, the CO_2 flux was $-0.8\,\mu mol\,m^{-2}\,s^{-1}$ at the end of the immersion and rose to 3.0 $\mu mol\,m^{-2}\,s^{-1}$ at the beginning of emersion (Fig. 4e). There are a number of processes that can induce these rapid changes in NEE, including benthic and planktonic GPP and CR, advection with water movements and air-water gas exchange. Although in the intertidal Wadden Sea, Zemmelink et al. (2009) found little dependency of CO_2 fluxes on the tide, this was not the case in the Arcachon lagoon. The effect of rising tide on CO_2 exchange was first reported by Houghton and Woodwell (1980) in a salt marsh. Kathilankal et al. (2008) reported a 46 % reduction in CO_2 uptake during emersion. In these salt marsh systems, part of the vegetation remains emerged even at high tide. In intertidal systems like the Arcachon lagoon or the Wadden Sea, at low tide, benthic GPP and CR are theoretically the two main drivers of NEE (i.e., NEP in this case), as discussed in the previous section. When the tide rises over the flat, benthic and planktonic communities contribute to GPP and CR, but their effect on NEE may not be immediate because water–air gas exchange is slow in comparison with the duration of the immersion. For instance, for typical conditions in coastal systems and a gas-transfer velocity of 10 $cm\,h^{-1}$, it takes 3.5 h for pCO_2 to decrease from 600 to 500 ppmv with gas exchange, which corresponds to a CO_2 flux of

BGD
8, 5451–5503, 2011

$\sim$1.2 µmol m^{-2} s^{-1}, comparable to what we observed here. Consequently, a negative water-air gradient can be created, for instance by phytoplankton at the mouth of the lagoon at low tide. When these undersaturated water masses enter the lagoon with the flood tide, a negative NEE would be observed, but it would be only partly the result of the NEP of the lagoon at high tide. Inversely, intense benthic and planktonic CR at high tide in the lagoon would not necessarily immediately generate an equivalent degassing of CO_2 to the atmosphere, with some of the CO_2 remaining in solution and being advected with the subsequent ebb tide. Such CO_2 outwelling from intertidal systems to adjacent creeks and bays has been observed in many tidal wetlands (Cai et al., 2003; Borges et al., 2003; Wang and Cai, 2004).

The September 2007 measurements at Station 2 in the inner part of the lagoon provide a first and relatively simple scheme for conceptualising NEE dynamics in relation to NEP at the different phases of the day and the tide. During this experiment, we observed strong CO_2 uptake at LT/day but CO_2 degassing during all other cases (Fig. 3e, Table 1). This suggests that at LT/day, the tidal flat was autotrophic, whereas it was heterotrophic during the night and during immersion. In addition, CO_2 degassing at LT/Night and HT/Night was significantly higher ($p < 0.05$) than at HT/day, which suggests that in the daytime, benthic and planktonic GPP could significantly reduce CO_2 degassing. Benthic GPP by microphytobenthos is controlled by light availability (Parsons et al., 1984) and is believed to be light limited during immersion. However, the presence of microphytobenthos can significantly contribute to planktonic GPP at the beginning of the flood tide. Indeed, Guarini (1998) showed that a large part of microphytobenthic cells can be re-suspended with the flooding tide and largely contribute to the planktonic GPP during HT/Day cases. In September 2007 at Station 2, we found a significant positive correlation between CO_2 fluxes and water height (Fig. 9). Indeed, the lagoon clearly shifted from a sink of CO_2 at LT/day (Table 1) to a source of CO_2 to the atmosphere with the rising tide as soon as the water height reached 0.5 m. It is possible that during this transition phase the organic matter newly synthesised by the microphytobenthos, predominant at this station at low tide, fed the respiration of

BGD
8, 5451–5503, 2011

the water column during high tide. Such rapid carbon recycling between the benthic and planktonic compartments would explain the NEE patterns observed during this experiment.

At Station 1, in the centre of the lagoon, patterns of CO_2 fluxes were fundamentally different, as uptake of atmospheric CO_2 were also observed during immersion. This was the case during the day at the three periods of measurements and also during the night in September 2008 and in April 2009. In contrast, in July 2008, the lagoon was a source of CO_2 at HT/Night, being a sink at HT/Day (Table 1). Negative NEE during HT/Night demonstrates the impact of planktonic GPP at the outlet of the lagoon, followed by advection of CO_2-depleted water masses with the flood tide. Indeed, the channel and subtidal areas of the lagoon are the sites of development of phytoplankton blooms in the lagoon dominated by large diatom cells leading to high primary production rates, particularly in early spring (Glé et al., 2007, 2008). In April 2009, the uptake of atmospheric CO_2 during immersion at Station 1 was nearly two times higher at night than during the day (Table 1), which reveals that the CO_2 depletion of the waters occurred a few hours before daytime, precisely when the water masses were at the mouth of the lagoon. On the contrary, the water present at daytime over the tidal flat absorbed less atmospheric CO_2, as it was present at the outlet of the lagoon during the night; this also suggests that during this spring period, GPP during immersion was lower in the lagoon than outside of the lagoon. Glé et al. (2007) showed that, in late winter–early spring (in 1999 and 2003) at each high tide during this season, oceanic blooms were advected into the lagoon, first in the external waters and second in the internal waters, with the intensity of this production being always higher in the external waters. In addition, in spring 2009 at Station 1, as previously discussed, microphytobenthic GPP was important during the LT/Day case; we thus expected that, like in autumn 2007 at Station 2, the exudation of highly biodegradable compounds to the water would enhance CR during the following immersion phase (Guarini, 1998). However, we did not observe CO_2 degassing during this phase, but rather negative or slightly positive NEE. This suggests that at this season, the respired microphytobenthic GPP could participate in

BGD
8, 5451–5503, 2011

the decrease observed in the CO_2 uptake from LT/Day to HT/Day (Table 1) but that planktonic GPP dominates during the immersion phase at Station 1.

In July and September 2008, NEE during emersion at Station 1 showed different patterns. In September, NEE was slightly negative ($\sim -0.2\,\mu mol\,m^{-2}\,s^{-1}$; Table 1) at both HT/Day and HT/Night, suggesting a predominant role of advection of CO_2-depleted waters from the mouth of the lagoon, as in April 2009. In contrast, in July 2008, the water in the lagoon was a sink of CO_2 at daytime but a source of CO_2 at night, meaning that advection phenomena were probably less important than metabolic processes in the lagoon at Station 1 (Table 1).

CO_2 uptake at LT/Day was systematically reduced at HT/Day during the four deployments (Fig. 5e and Table 1). CO_2 uptakes could be reduced by the lower photosynthetic activity of primary producers due to light limitation in the presence of water; this is especially true for *Zostera noltii* in the summer and autumn seasons in 2008 at Station 1, where the seagrass cover is maximal. However, Silva et al. (2005) noted that information on photosynthetic efficiency during air-exposed versus immersed conditions is inconsistent, suggesting that the key factor in CO_2 uptake by air-exposed *Zostera noltii* is the leaf water content (Silva et al., 2005). Leuschner et al. (1998) demonstrated a linear relationship between the leaf water content of the marine angiosperm and its net photosynthetic rate. In the Arcachon lagoon, the existence of depressions in the sediment at low tide probably allowed higher photosynthetic rates of the seagrass than during water immersion, as shown by Silva et al. (2005) in the Ria Formosa lagoon. Indeed, these depressions could retain a considerable amount of water, enough to maintain leaf hydration, and allow rapid air-water CO_2 diffusion. Nevertheless, even if CO_2 diffuses through water approximately 10000-fold more slowly than through air (Stumm and Morgan, 1996), carbon uptake continues during tidal flooding in the lagoon but at reduced rates, as shown by the CO_2 uptake generally still measured at this case for the four deployments (Table 1). In addition, the decrease in CO_2 uptake during the day, along with the CO_2 degassing to the atmosphere at night (Fig. 5e) with the tide, can also result from physical processes, with the water column acting as a diffusion

BGD
8, 5451–5503, 2011

barrier against gas exchange between the water and the atmosphere (Houghton and Woodwell, 1980; Kathilankal et al., 2008). Other examples of physical processes driving CO_2 fluxes were discussed in Polsenaere et al. (2011), i.e., at Station 1, in July 2008 on Day 184 (Fig. 4e), and also in the present study in September–October 2008 on Day 279 (Fig. 5e). In both periods, a strong CO_2 degassing to the atmosphere was measured at LT/Day. The singular CO_2 degassing, too high and rapid to be explained by biological respiration, could be attributed to destocking processes linked to the onset of atmospheric turbulence (high wind speeds) occurring on some days, particularly in the morning or in the midday, after calm atmospheric conditions.

4.2 Tidal flats and the CO_2 budget of the coastal zone

Several studies have focused on CO_2 exchange with the atmosphere over coastal areas and have highlighted the dynamic and heterogeneity of these systems. Using pCO_2-based-flux calculations, benthic chambers or EC techniques, CO_2 budgets in various coastal environments have been reported. Concerning coastal wetlands, the study of Heilman et al. (1999), with a conditional sampling technique, reported carbon exchanges between a freshwater marsh in Texas (United States) and the atmosphere, from -1.9 to $1.7\,g\,C\,m^{-2}\,day^{-1}$. Using the EC method over a freshwater marsh dominated by *Typha latifolia* L. in California (United States), Rocha and Goulden (2008) reported a carbon release of $0.4\,g\,C\,m^{-2}\,day^{-1}$ averaged over five years of measurement between 1999 and 2003. In a salt marsh dominated by *Spartina alterniflora*, located on the eastern coast of Virginia (United States), Kathilankal et al. (2008) measured, using an EC system, a carbon assimilation of $-0.7\,g\,C\,m^{-2}\,day^{-1}$ averaged over the six months corresponding to the growing season. Houghton and Woodwell (1980) measured a net flow of carbon of $-0.8\,g\,C\,m^{-2}\,yr^{-1}$ from the atmosphere to the Flax Pond salt marsh, dominated by *Spartina alterniflora*, on the north shore of Long Island, New York (United States). Concerning tidal flats, Zemmelink et al. (2009) computed a carbon uptake from the atmosphere to an intertidal estuary of the Wadden Sea (Griend Island, Netherlands) of $-1.9\,g\,C\,m^{-2}\,day^{-1}$ averaged over 68 days of measurements

BGD
8, 5451–5503, 2011

during the spring period. Spilmont et al. (2006), using the benthic chamber technique, reported a low autotrophic carbon budget of $-0.1\,g\,C\,m^{-2}\,day^{-1}$ for the mudflat of the Seine estuary (English Channel, France). Finally, in the Bay of Somme (Eastern English Channel, France), Migné et al. (2004), using the same method, computed a heterotrophic carbon budget of $0.2\,g\,C\,m^{-2}\,day^{-1}$ at maximum.

Because we do not have flux data for winter conditions, we will not attempt to provide a precise annual CO_2 budget for the Arcachon lagoon. However, the estimation given here takes into account the most productive seasons of the bay over three years, i.e., spring, summer and early autumn, as well as the spatial variations in CO_2 fluxes existing in the tidal flat, i.e., with measurements in two different stations. Thus, our data reveal that in spring, the lagoon represented a net sink of CO_2 of $-2.5\,g\,C\,m^{-2}\,day^{-1}$, whereas in summer and early autumn, the lagoon either acted as a small source or sink of CO_2, with 0.1 and $-0.2 \sim 0.8\,g\,C\,m^{-2}\,day^{-1}$, respectively. This carbon uptake is similar to or greater than those computed in the other tidal flats in France and in Netherlands (Migné et al., 2004; Spilmont et al., 2006; Zemmelink et al., 2009). Nevertheless, it remained low compared to other tidal systems, such as salt or freshwater marshes (Houghton and Woodwell, 1980; Rocha and Goulden, 2008) or temperate estuaries (Frankignoulle, 1998).

Even if annual fluxes of atmospheric CO_2 over lagoons are relatively weak, these latter remain sparsely characterised from a carbon budget perspective. In the last evaluation of carbon fluxes in the global ocean carried out by Laruelle et al. (2010), studies on carbon fluxes over lagoons account for only 10 % of the global flux. However, the intertidal area represents 24 % of the surface area of the estuarine environment surface. In addition, CO_2 fluxes in tidal flats and estuaries are greatly contrasting, with estuarine water emitting large amounts of CO_2, whereas the intertidal area absorbs CO_2 in small quantities. In consequence, separating tidal flats from the rest of estuarine systems would reduce the global CO_2 emission by near-shore estuarine environments computed by Laruelle et al. (2010).

BGD
8, 5451–5503, 2011

Acknowledgements. This study was supported by the ANR project PROTIDAL coordinated by Pierre Anschutz and also by the Aquitaine region that has financed the EC system. We are grateful to Guillaume Detandt, Georges Oggian and Dominique Serça for their help for the EC deployment. We acknowledge the Kalideos teams for giving us access the satellite image database.

The publication of this article is financed by CNRS-INSU.

References

Abril, G., Etcheber, H., Delille, B., Frankignoulle, M., and Borges, A. V.: Carbonate dissolution in the turbid and eutrophic Loire estuary, Mar. Ecol.-Prog. Ser., 259, 129–138, 2003.

Amanieu, M.: Recherches écologiques sur la faune des plages abritées et des étangs saumâtres de la région d'Arcachon, Ph.D. thesis, Université Bordeaux 1, 234 pp., 1967.

Auby, I.: Contribution à l'étude des herbiers de *zostera noltii* dans le bassin d'Arcachon, Ph.D. thesis, Université Bordeaux 1, 234 pp., 1991.

Auby, I. and Labourg, P. J.: Seasonal dynamics of Zostera noltii Hornem in Bay of Arcachon (France), J. Sea Res., 35, 269–277, 1996.

Aubinet, M., Grelle, A., Ibrom, A., Rannik, U., Moncrieff, J., Foken, T., Kowalski, A. S., Martin, P. H., Berbigier, P., Bernhofer, C. H., Clement, R., Elbers, J., Granier, A., Grunwald, T., Morgenstern, K., Pilegaard, K., Rebmann, C., Snijders, W., Valentini, R., and Vesala, T.: Estimates of the annual net carbon and water exchange of European forests: the EUROFLUX methodology, Adv. Ecol. Res., 30, 113–175, 2000.

Baldocchi, D. D., Hincks, B. B. and Meyers, T. P.: Measuring biosphere-atmosphere exchanges of biologically related gases with micrometeorological methods, Ecology, 5, 1331–1340, 1988.

BGD
8, 5451–5503, 2011

Baldocchi, D. D.: Assessing the eddy covariance technique for evaluating carbon dioxide exchange rates of ecosystems: past, present and future, Glob. Change Biol., 9, 479–492, 2003.
Barillé, L., Robin, M., Harin, N., Bargain, A., and Launeau, P.: Increase in seagrass distribution at Bourgneuf Bay (France) detected by spatial remote sensing, Aquat. Bot., 92, 185–194, 2010.
Barrón, C., Duarte, C. M., Frankignoulle, M., and Borges, A. V.: Organic carbon metabolism and carbonate dynamics in a Mediterranean seagrass (*Posidonia oceanica*) meadow, Estuar. Coast., 29, 417–426, 2006.
Blanchard, G. F. and Cariou-Le Gall, V.: Photosynthetic characteristics of microphytobenthos in Marennes-Oléron Bay, France: preliminary results, J. Exp. Mar. Biol. Ecol., 182, 1–14, 1994.
Blanchard, G. F., Guarini, J. M., Orvain, F., and Sauriau, P. G.: Dynamic behaviour of benthic microalgal biomassin intertidal mudflats, J. Exp. Mar. Biol. Ecol., 264, 85–100, 2001.
Blanchard, G. F., Guarini, J. M., Dang, C., and Richard, P.: Characterizing and quantify photoinhibition in intertidal microphytobenthos, J. Phycol., 40, 692–696, 2004.
Borges, A. V.: Do we have enough pieces of the jigsaw to integrate CO_2 fluxes in the coastal ocean?, Estuaries, 28, 3–27, 2005.
Borges, A. V., Djenidi, S., Lacroix, G., Théate, J., Delille, B., and Frankignoulle, M.: Atmospheric CO_2 flux from mangrove surrounding waters, Geophys. Res. Lett., 30(11), 1558, doi:10.1029/2003GL017143, 2003.
Borges, A. V., Delille, B., and Frankignoulle, M.: Budgeting sinks and sources of CO_2 in the coastal ocean: diversity of ecosystems counts, Geophys. Res. Lett., 32, L14601, doi:10.1029/2005GL023053, 2005.
Borges, A. V., Schiettecatte, L.-S., Abril, G., Delille, B., and Gazeau, F.: Carbon dioxide in European coastal waters, Estuar. Coast. Shelf S., 70, 375–387, 2006.
Burba, G. and Anderson, D.: Introduction to the Eddy Covariance method: General Guidelines and Conventional Workflow, Licor, Inc., 1–141, 2005.
Cai, W.-J., Wang, Z., and Wang, Y.: The role of marsh-dominated heterotrophic continental margins in transport of CO_2 between the atmosphere, the land-sea interface and the ocean, Geophys. Res. Lett., 30, 1849, doi:10.1029/2003GL017633, 2003.
Chapin, F. S., Woodwell, G. M., Randerson, J. T., Rastetter, E. B., Lovett, G. M., Baldocchi, D. D., Clark, A., Harmon, M. E., Schimel, D. S., Valentini, R., Wirth, C., Aber, J. D., Cole, J. J., Goulden, M. L., Harden, J. W., Heimann, M., Howarth, R. W., Matson, P. A., McGuire,

BGD
8, 5451–5503, 2011

A. D., Melillo, J. M., Mooney, H. A., Neff, J. C., Houghton, R. A., Pace, M. L., Ryan, M. G., Running, S. W., Sala, O. E., Schlesinger, W. H., and Schulze, E. D.: Reconciling Carbon-cycle Concepts, Terminology, and Methods, Ecosystems, 9, 1041–1050, 2006.

Chauvaud, L., Thompson, J. K., Cloern, J. E., and Thouzeau, G.: Clams as CO_2 generators: The *Potamocorbula amurensis* example in San Francisco Bay, Limnol. Oceanogr., 48, 2086–2092, 2003.

Den Hartog, C.: The sea-grasses of the world, Verh. Kon. Ned. Akad. Wet. Afd. Natuurk., Reeks 2, 59(1), 1–275, 1970.

De Wit, R., Leibreich, J., Vernier, F., Delmas, F., Beuffe, H., Maison, Ph., Chossat, J. C., Laplace-Treyture, C., Laplana, R., Clavé, V., Torre, M., Auby, I., Trut, G., Maurer, D., and Capdeville, P.: Relationship between land-use in the agro-forestry system of les Landes, nitrogen loading to and risk of macro-algal blooming in the bassin d'Arcachon coastal lagoon (sw France), Estuar. Coast. Shelf S., 62, 453–465, 2005.

Duarte, C. M.: Temporal biomass variability and production/biomass relationships of seagrass communities, Mar. Ecol.-Prog. Ser., 51, 269–276, 1989.

Duarte, C. M., Marbà, N., Gacia, E., Fourqurean, J. W., Beggins, J., Barrón, C., and Apostolaki, E. T.: Seagrass community metabolism: assessing the carbon sink capacity of seagrass meadows, Global Biogeochem. Cy., 24, 1–8, 2010.

Foken, T.: Angewandte Meteorologie, Mikrometeorologische Methoden, Springer, Heidelberg, 289 pp., 2003.

Foken, T. and Wichura, B.: Tools for quality assessment of surface-based flux measurements, Agr. Forest Meteorol., 78, 83–105, 1996.

Foken, T., Skeib, G., and Richter, S. H.: Dependence of the integral turbulence characteristics on the stability of stratification and their use for Doppler-Sodar measurements, Z. Meteorol., 41, 311–315, 1991.

Frankignoulle, M., Abril, G., Borges, A. V., Bourge, I., Canon, C., Delille, B., Libert, E., and Théate, J. M.: Carbon dioxide emission from European estuaries, Science, 282, 434–436, 1998.

Frankignoulle, M., Biondo, R., Théate, J.-M., and Borges, A. V.: Carbon dioxide daily variations and atmospheric fluxes over the open waters of the Great Bahama Bank and Norman's Pond using a novel autonomous measuring system, Caribb. J. Sci., 39, 257–264, 2003.

Gattuso, J.-P., Frankignoulle, M., and Wollast, R.: Carbon and carbonate metabolism in coastal aquatic systems, Annual Review Ecology Systematics, 29, 405–433, 1998.

BGD
8, 5451–5503, 2011

Gazeau, F., Smith, V. S., Gentili, B., Frankignulle, M., and Gattuso, J. P.: The European coastal zone: characterization and first assessment of ecosystem metabolism, Estuar. Coast. Shelf S., 60, 673–694, 2004.
Guarini, J. M.: Modélisation de la dynamique du microphytobenthos des vasières intertidales du bassin de Marennes-Oléron, Ph.D. thesis, Université Pierre et Marie Curie, 177 pp., 1998.
Glé, C., Amo, Y. D., Bec, B., Sautour, B., Froidefond, J. M., Gohin, F., Maurer, D., Plus, M., Laborde, P., and Chardy, P.: Typology of environmental conditions at the onset of winter phytoplankton blooms in a shallow macrotidal coastal ecosystem, Arcachon Bay (France), J. Plankton Res., 29, 999–1014, 2007.
Glé, C., Amo, Y. D., Sautour, B., Laborde, P., and Chardy, P.: Variability of nutrients and phytoplankton primary production in a shallow macrotidal coastal ecosystem Arcachon Bay, France, Estuar. Coast. Shelf S., 76, 642–656, 2008.
Heilman, J. L., Cobos, D. R., Heinsch, F. A., Campbell, C. S., and McInnes, K. J.: Tower-based conditional sampling for measuring ecosystem-scale carbon dioxide exchange in coastal wetlands, Estuaries, 22, 584–591, 1999.
Houghton, R. A. and Woodwell, G. M.: The Flax Pond ecosystem study: exchanges of CO_2 between a salt marsh and the atmosphere, Ecology, 61, 1434–1445, 1980.
Hsieh, C. I., Katul, G., and Chi, T. W.: An approximate analytical model for footprint estimation of scalar fluxes in thermally stratified atmospheric flows, Adv. Water Resour., 23, 765–772, 2000.
Hubas, C., Davoult, D., Cariou, T., and Artigas, L. P.: Factors controlling benthic metabolism during low tide along a granulometric gradient in an intertidal bay (Roscoff Aber Bay, France), Mar. Ecol.-Prog. Ser., 316, 53–68, 2006.
Kaimal, J. C., Wyngaard, J. C, Izumi, Y., and Cote, O. R.: Spectral characteristics of surface layer turbulence, Q. J. Roy. Meteor. Soc., 98, 563–589, 1972.
Kathilankal, J. C., Mozdzer, T. J., Fuentes, D., D'Odorico, P., McGlathery, K. J., and Zieman, J. C.: Tidal influences on carbon assimilation by a salt marsh, Environ. Res. Lett., 3, 1–6, 2008.
Laruelle, G. G, Dürr, H. H., Slomp, C. P., and Borges, A. V.: Evaluation of sinks and sources of CO_2 in the global coastal ocean using a spatially-explicit typology of estuaries and continental shelves, Geophys. Res. Lett., 37, L15607, doi:10.1029/2010GL043691, 2010.
Leclerc, M. Y. and Thurtell, G. W.: Footprint prediction of scalar fluxes using a Markovian analysis, Bound.-Lay. Meteorol., 52, 247–258, 1990.

BGD
8, 5451–5503, 2011

Leuschner, C., Landwehr, S., and Mehlig, U.: Limitation of carbon assimilation of intertidal *Zostra noltii* and *Z. marina* by dessication at low tide, Aquat. Bot., 62, 171–176, 1998.
Manaud, F., Bouchet, J. M., Deltreil, J. P., Maurer, D., Trut, G., Auby, I., Dreno, J. P., L'Yavanc, J., Masson, N., and Pellier, C.: Etude intégrée du Bassin d'Arcachon. Tome 1: Physique. Activités ressources vivantes, Rapport Interne DEL/Arcachon, 1997.
Mantoura, R. F. C., Martin, J. M., and Wollast, R.: Ocean margin processes, in: Global Change, Chichester, UK: Wiley & Sons, 469 pp., 1991.
McRoy, C. P. and McMillan, C.: Production ecology and physiology of seagrasses, in: Production Ecology and Physiology of Seagrasses, edited by: McRoy, C. P. and Helferrich, C., Dekler, New York, USA, 58–87, 1977.
Middelburg, J. J., Barranguet, C., Boschker, H. T. S., Hermann, P. M. J., Moens, T., and Heip, C. H. R.: The fate of intertidal microphytobenthos carbon: an *in situ* ^{13}C-labeling study, Limnol. Oceanogr. 45, 1224–1234, 2000.
Migné, A., Davoult, D., Spilmont, N., Boucher, G., Gattuso, J. P., and Rybarczyk, H.: A closed-chamber CO_2 flux method for estimating primary production and respiration under emersed conditions, Mar. Biol., 140, 865–869, 2002.
Migné, A., Spilmont, N., and Davoult, D.: *In situ* measurements of benthic primary production during emersion: seasonal variations and annual production in the Bay of Somme (eastern English Channel, France), Cont. Shelf Res., 24, 1437–1449, 2004.
Migné, A., Gévaert, F., Créach, A., Spilmont, N., Chevalier, E., and Davoult, D.: Photosynthetic activity of intertidal microphytobenthic communities during emersion: in situ measurements of Chlorophyll fluorescence (PAM) and CO_2 flux (IRGA), J. Phycol., 43, 864–873, 2007.
Moncrieff, J.-B., Massheder, J. M., de Bruin, H., Elbers, J., Friborg, T., Heusinkveld, B., Kabat, P., Scott, S., Soegaard, H., and Verhoef, A.: A system to measure surface fluxes of momentum, sensible heat, water vapour and carbon dioxide, J. Hydrol., 188–189, 589–611, 1997.
Moore, C. J.: Frequency response corrections for eddy correlation systems, Bound.-Lay. Meteorol., 37, 17–35, 1986.
Morison, J. I. L., Piedade, M. T. F, Müller, E., Long, S. P., Junk, W. J., and Jones, M. B.: Very high productivity of the C_4 aquatic grass *Echinochloa polystachya* in the Amazon floodplain confirmed by net ecosystem CO_2 flux measurements, Oecologia, 125, 400–411, 2000.
Odum, H. T.: Primary production in flowing waters, Limnol. Oceanogr., 1, 102–117, 1956.
Ouisse, V., Migne, A., and Davoult, D.: Seasonal variations of community production,

BGD
8, 5451–5503, 2011

respiration and biomass of different primary producers in an intertidal Zostera noltii bed (Western English Channel, France), Hydrobiologia, 649, 3–11, 2010.
Parsons, T. R., Takahashi, M., and Hargrave, B.: Biological Oceanographic Processes, 3rd edn., Pergamon Press Ltd, Oxford, 330 pp., 1984.
Pernetta, J. C and Milliman, J. D.: Land-Ocean interactions in the coastal zone, Implementation plan, IGPB Rep., 33, 1–215, 1995.
Plus, M., Stanisière, J.-Y., Maurer, D., and Dumas, F.: Etude comparative des composantes hydrodynamiques de deux systèmes côtiers mésotidaux, les Bassins d'Arcachon et de Marennes-Oléron, Rapport commun LER-AR/LER-PC/DYNECO PHYSED, Ifremer, 1–25, 2008.
Plus, M., Dalloyau, S., Trut, G., Auby, I., de Montaudouin, X., Emery, E., Noël, C., and Viala, C.: Long-term evolution (1988–2008) of *Zostera* spp. Meadows in Arcachon bay (Bay of Biscay), Estuar. Coast. Shelf S., 87, 357–366, 2010.
Polsenaere, P., Lamaud, E., Bretel, P., Bonnefond, J. M., Delille, B., Detandt, G., Loustau, D., and Abril, G.: Turbulent flux measurements by Eddy Correlation over a temperate intertidal flat in the southwest of France, J. Geophys. Res., submitted, 2011.
Raymond, P. A. and Cole, J. J.: Gas exchange in rivers and estuaries: choosing a gas transfer velocity, Estuaries, 24, 312–317, 2001.
Rimmelin, P., Dumon, J. C., Maneux, E., and Gonçalves, A.: Study of annual and seasonal dissolved inorganic nitrogen inputs into the Arcachon lagoon, Atlantic coast (France). Estuar. Coast. Shelf S., 47, 649–659, 1998.
Rocha, A. V. and Goulden, M. L.: Large interannual CO_2 and energy exchange variability in a freshwater marsh under consistent environmental conditions, J. Geophys. Res., 113, 1–12, G04019, 2008.
Serôdio, J., Vieira, S., and Cruz, S.: Photosynthetic activity, photoprotection and photoinhibition in intertidal microphytobenthos as studied in situ using variable chlorophyll fluorescence, Cont. Shelf Res., 28, 1363–1375, 2008.
Silva, J., Santos, R., Calleja, M. Ll., and Duarte, C. M.: Submerged versus air-exposed intertidal macrophyte productivity: from physiological to community-level assessments, J. Exp. Mar. Biol. Ecol., 317, 87–95, 2005.
Smith, S. V. and Hollibaugh, J. T.: Coastal metabolism and the ocean organic carbon balance, Rev. Geophys., 31, 75–89, 1993.
Spilmont, N., Davoult, D., and Migné, A.: Benthic primary production during emersion: in

BGD
8, 5451–5503, 2011

situ measurements and potential primary production in the Seine Estuary (English Channel, France), Mar. Pollut. Bull., 54, 49–55, 2006.
Stum, W. and Morgan, J. J.: Aquatic chemistry: chemical equilibria and rates in natural waters, 3rd edn., Wiley-Interscience, New York, 1996.
Vachon, D., Prairie, Y. T., and Cole, J. J.: The relationship between near-surface turbulence and gas transfer velocity in freshwater systems and its effect on floating chamber measurements, Limnol. Oceanogr., 55(4), 1723–1732, 2010.
Vermaat, J. E. and Verhagen, F. C. A.: Seasonal variation in the intertidal seagrass *Zostera noltii* Hornem.: coupling demographic and physiological patterns, Aquat. Bot., 52, 259–281, 1996.
Wang, Z. A. and Cai, W.-J.: Carbon dioxide degassing and inorganic carbon export from a marsh-dominated estuary (the Dublin River): a marsh CO_2 pump, Limnol. Oceanogr., 49, 341–354, 2004.
Webb, E. K., Pearman, G., and Leuning, R.: Correction of flux measurements for density effects due to heat and water vapour transfer, Q. J. Roy. Meteor. Soc., 106, 85–100, 1980.
Zemmelink, H. J., Slagter, H. A., van Slooten, C., Snoek, J., Heusinkveld, B., Elbers, J., Bink, N. J., Klaassen, W., Philippart, C. J. M., and de Baar, H. J. W.: Primary production and eddy correlation measurements of CO_2 exchange over an intertidal estuary, Geophys. Res. Lett., 36, LI19606, doi:10.1029/2009GL039285, 2009.

BGD
8, 5451–5503, 2011

Table 1. Carbon dioxide fluxes (F_c) measured in the Arcachon lagoon in September/October 2007 at Station 2 and July 2008, September/October 2008 and April 2009 at Station 1 (see Fig. 1). Negative fluxes represent sinks of CO_2 and positive fluxes represent sources of CO_2 to the atmosphere by convention. A PAR threshold of 20 µmol m^{-2} s^{-1} has been chosen to separate day and night cases and low tide cases corresponding to zero-water heights.

F_c (µmol m^{-2} s^{-1})	Low Tide/Day	Low Tide/Night	High Tide/Day	High Tide/Night	Average F_c	Daily F_c
September/October 2007 (Station 2)	−1.7 ± 1.70 (−10.0 ~ 0.9)	2.7 ± 3.7 (0.2 ~ 18.6)	0.4 ± 1.1 (−2.4 ~ 3.9)	1.9 ± 2.4 (−0.4 ~ 13.3)	0.8 ± 2.7 (−10.0 ~ 18.6)	0.5 ± 0.4 (0.1 ~ 1.0)
July 2008 (Station 1)	−0.31 ± 3.29 (−5.75 ~ 12.00)	0.9 ± 0.8 (−2.5 ~ 3.1)	−0.2 ± 1.4 (−5.0 ~ 7.3)	0.7 ± 1.9 (−2.8 ~ 10.6)	0.1 ± 1.9 (−5.7 ~ 12.0)	0.1 ± 0.9 (0.8 ~ 3.1)
September/October 2008 (Station 1)	−0.7 ± 2.3 (−10.8 ~ 14.3)	0.2 ± 1.1 (−7.1 ~ 5.3)	−0.14 ± 0.66 (−5.91 ~ 3.43)	−0.27 ± 1.32 (−7.49 ~ 4.51)	−0.23 ± 1.44 (−10.77 ~ 14.30)	−0.23 ± 0.68 (−1.19 ~ 1.20)
April 2009 (Station 1)	−2.7 ± 2.0 (−11.7 ~ 0.6)	−1.3 ± 1.4* (−6.2 ~ 1.9)	−1.7 ± 1.4 (−8.7 ~ 2.6)	−3.2 ± 2.4 (−13.1 ~ 0.4)	−2.4 ± 2.1 (−13.1 ~ 2.6)	−2.4 ± 0.9 (−4.2 ~ −0.8)

* Negative F_c data corresponding to very short periods of low tide/night and very fast changes in CO_2 fluxes in April 2009 (Days 94 and 96, Fig. 6e) were excluded from the average, as they were potentially affected by flooded areas.

BGD
8, 5451–5503, 2011

Table 2. Relationships between the *Zostera noltii* cover from the satellite image analyses and the measured CO_2 fluxes from the Arcachon lagoon, at low tide during the day, according to sectors of wind direction. 0–45°: north-northeast, 45–90°: east-northeast, 90–135°: east-southeast, 135–180°: south-southeast, 180–225°: south-southwest; 225–270°: west-southwest, 270–315°: west-northwest, 315–360°: north-northwest wind directions. Notice that F_c values obtained in July 2008 during the beginning of the experiment (Days 183, 184) and in September–October 2008 (Day 279) have been discarded for calculations, representing destocking but not biological degassing by respiration (Figs. 5f and 6f).

		NNE 0–45°	ENE 45–90°	ESE 90–135°	SSE 135–180°	SSW 180–225°	WSW 225–270°	WNW 270–315°	NNW 315–360°
Station 2 Autumn 2007	*Zostera noltii* cover (13 Sep 2007)	19 %	25 %	27 %	17 %	4 %	14 %	15 %	51 %
	F_c (μmol m^{-2} s^{-1})		−0.9 ± 0.7	−2.1 ± 1.4	−2.1 ± 4.4	−0.7 ± 0.6	−0.7 ± 0.7		
	Percentage of F_c data		4 %	61 %	7 %	21 %	7 %		
Station 1 Summer 2008	F_c (μmol m^{-2} s^{-1})			−1.1 ± 0.9	−1.4 ± 0.3	−1.4 ± 0.6	−0.9 ± 0.9	−2.0 ± 1.4	−0.7 ± 0.2
	Percentage of F_c data			11 %	6 %	14 %	18 %	47 %	4 %
Station 1 Autumn 2008	*Zostera noltii* cover (17 Oct 2008)	98 %	93 %	86 %	70 %	95 %	99 %	99 %	98 %
	Zostera noltii cover (8 Sep 2009)	97 %	95 %	87 %	69 %	94 %	98 %	99 %	98 %
	F_c (μmol m^{-2} s^{-1})	−0.5 ± 1.5	−0.7 ± 1.3	−0.1 ± 0.9	−0.9 ± 1.0	−1.5 ± 2.6	−2.2 ± 2.0	−2.0 ± 1.1	−1.5 ± 1.2
	Percentage of F_c data	9 %	17 %	14 %	21 %	9 %	6 %	12 %	12 %
Station 1 Spring 2009	*Zostera noltii* cover (24 Jun 2009)	90 %	89 %	74 %	62 %	94 %	97 %	96 %	94 %
	F_c (μmol m^{-2} s^{-1})			−3.8 ± 3.6	−1.0 ± 1.6	−1.6 ± 1.0	−4.5 ± 2.6	−3.0 ± 1.5	−3.1 ± 1.2
	Percentage of F_c data			6 %	19 %	8 %	7 %	32 %	28 %

BGD
8, 5451–5503, 2011

Table 3. Comparison of NEP components at low tide for the autumn season at the two stations and in summer at Station 1. NEP was assumed as NEE at low tide during daytime, CR was assumed as NEE at low tide during the night, and GPP was assumed as the sum of NEP and CR. Notice that F_c values obtained in July 2008 during the beginning of the experiment (Days 183, 184) and in September-October 2008 (Day 279) have been discarded for calculations, representing destocking but not biological degassing by respiration (Figs. 5f and 6f). The GPP and CR calculations for the spring 2009 period at Station 1 were not possible because of the slight negative averaged flux value obtained at low tide/night.

	Zostera noltii cover (%)	NEP ($\mu mol\, m^{-2}\, s^{-1}$)	CR ($\mu mol\, m^{-2}\, s^{-1}$)	GPP ($\mu mol\, m^{-2}\, s^{-1}$)
September/October 2007 (Station 2)	22 ± 14	1.7 ± 1.7	2.7 ± 3.7	4.4
July 2008 (Station 1)		1.5 ± 1.2	1.0 ± 0.9	2.5
September/October 2008 (Station 1)	92 ± 10	0.9 ± 1.7	0.2 ± 1.1	1.1

BGD
8, 5451–5503, 2011

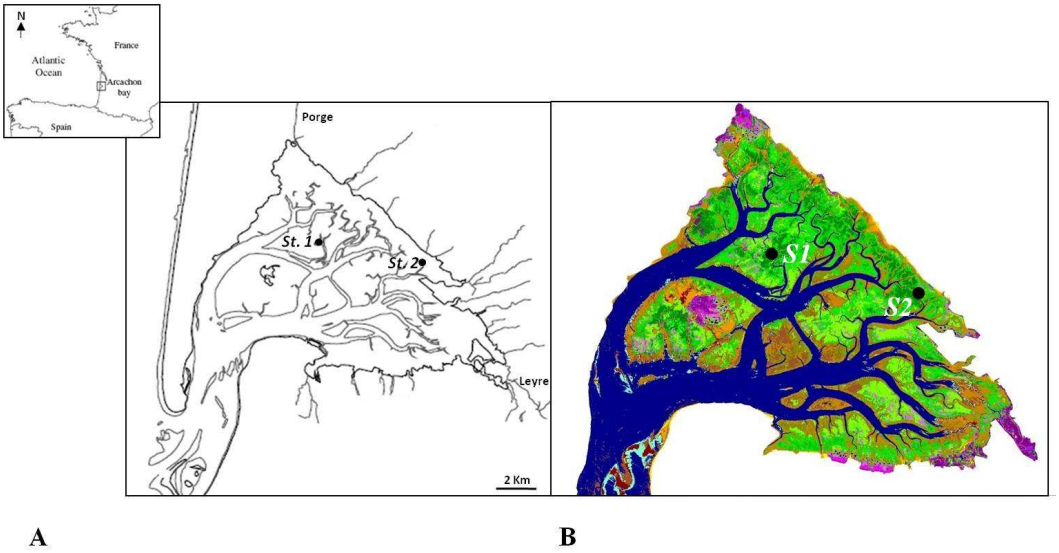

Fig. 1. Localisation and the Eddy Correlation (EC) experimental sites. **(A)**: the Arcachon lagoon with the subtidal zone (channels, in white) and the intertidal mudflat area (in grey); **(B)**: the two EC sites: Station 1 (44°42′59.15″ N, 01°08′36.96″ W) and Station 2 (44°42′19.96″ N, 01°04′01.35″ W). The *Zostera noltii* seagrass meadow is derived from the SPOT satellite image of the 22 June 2005; it represents 60 % of the intertidal area (shades of green show the differences in seagrass density).

BGD
8, 5451–5503, 2011

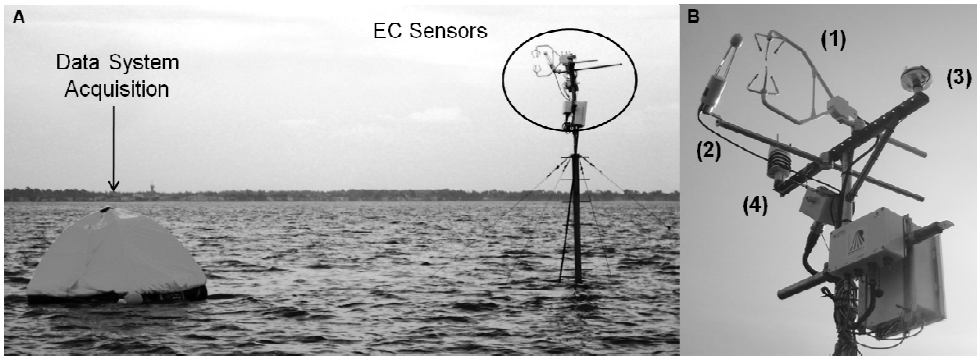

Fig. 2. The Eddy Correlation system deployed in the Arcachon lagoon in April 2009. **(A)**: general view of the system measurement showing the sensors mounted on the mast and the data system acquisition *Campbell CR3000* in the lifeboat; **(B)**: the sensors: (1) the sonic anemometer *CSAT3*, (2) the infra red gas analyser *LI-7500*, (3) the quantum sensor *SKP215* and (4) the meteorological station (*Vaisala WXT510*). The measurement heights were 4.20, 5.50, 7.0 and 5.0 m in September–October 2007, July 2008, September–October 2008 and April 2009, respectively.

BGD
8, 5451–5503, 2011

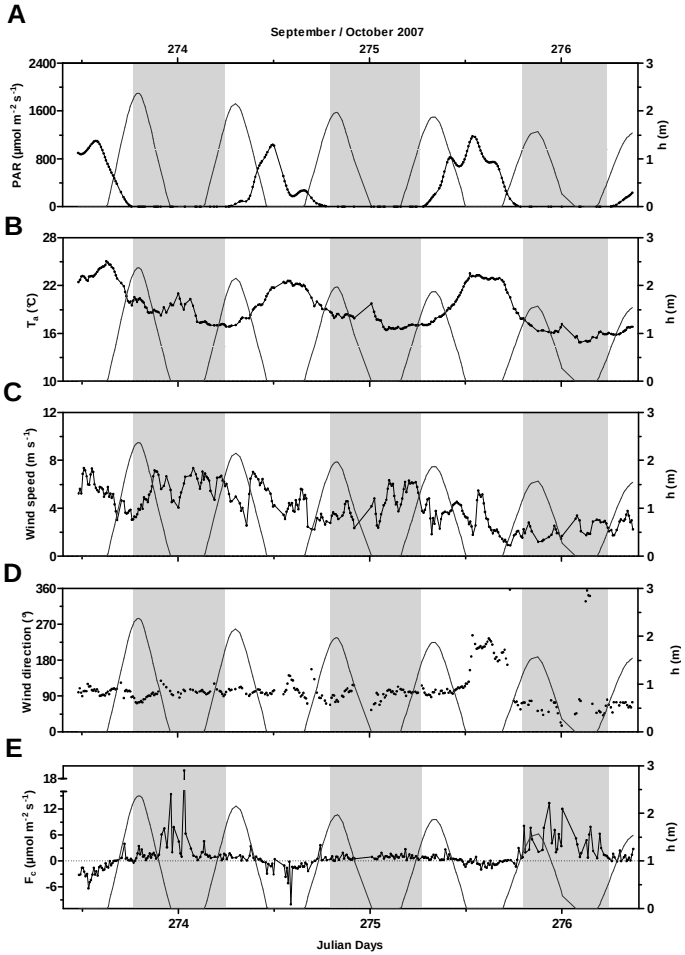

Fig. 3. (Caption on next page.)

BGD
8, 5451–5503, 2011

Fig. 3. Environmental parameters and carbon dioxide fluxes measured during the EC deployment in the Arcachon lagoon (St. 2) from 30 September at 11:35 to 3 October 2007 at 08:55 (GMT). **(A)**: photosynthetically active radiation ($\mu mol\,m^{-2}\,s^{-1}$) and water height (m); **(B)**: temperature of the air (°C); **(C)**: wind speed ($m\,s^{-1}$); **(D)**: wind direction (°) and **(E)**: carbon dioxide fluxes ($\mu mol\,m^{-2}\,s^{-1}$). Negative fluxes represent sinks of CO_2, and positive fluxes represent sources of $CO_2$to the atmosphere by convention. Day 273 squares with 30 September 2007. A PAR threshold of 20 $\mu mol\,m^{-2}\,s^{-1}$ was chosen to separate day and night cases, and low tide cases correspond to zero-water heights. PAR data have been transformed in $\mu mol\,m^{-2}\,s^{-1}$ from global radiation data in $W\,m^{-2}$, assuming a factor of 2 from global radiation to PAR values. A specific range for F_c (panel **E**) was chosen for a better visualisation of CO_2-flux variations.

BGD
8, 5451–5503, 2011

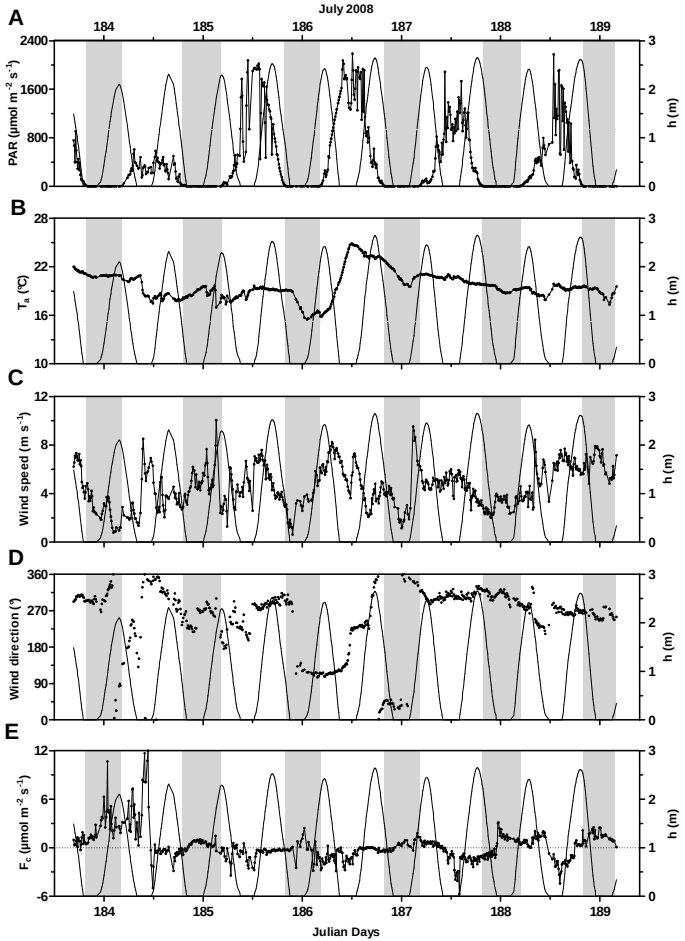

Fig. 4. (Caption on next page.)

BGD
8, 5451–5503, 2011

Fig. 4. Environmental parameters and carbon dioxide fluxes measured during the EC deployment in the Arcachon lagoon (St. 1) from 1 July at 16:40 to 7 July 2008 at 04:00 (GMT). **(A)**: photosynthetically active radiation PAR ($\mu mol\,m^{-2}\,s^{-1}$) and water height (m); **(B)**: temperature of the air (°C); **(C)**: wind speed ($m\,s^{-1}$); **(D)**: wind speed (°) and **(E)**: carbon dioxide fluxes ($\mu mol\,m^{-2}\,s^{-1}$). Negative fluxes represent sinks of CO_2, and positive fluxes represent sources of $CO_2$to the atmosphere by convention. Day 183 squares with 1 July 2008 and grey bands represent night periods. A PAR threshold of $20\,\mu mol\,m^{-2}\,s^{-1}$ was chosen to separate day and night cases, and low tide cases correspond to zero-water heights. Notice that four PAR data above $2200\,\mu mol\,m^{-2}\,s^{-1}$ are not shown, with the chosen scale corresponding to non-realistic data due to quantum sensor noise. A specific range for F_c (panel **E**) was chosen for a better visualisation of CO_2 flux variations.

BGD
8, 5451–5503, 2011

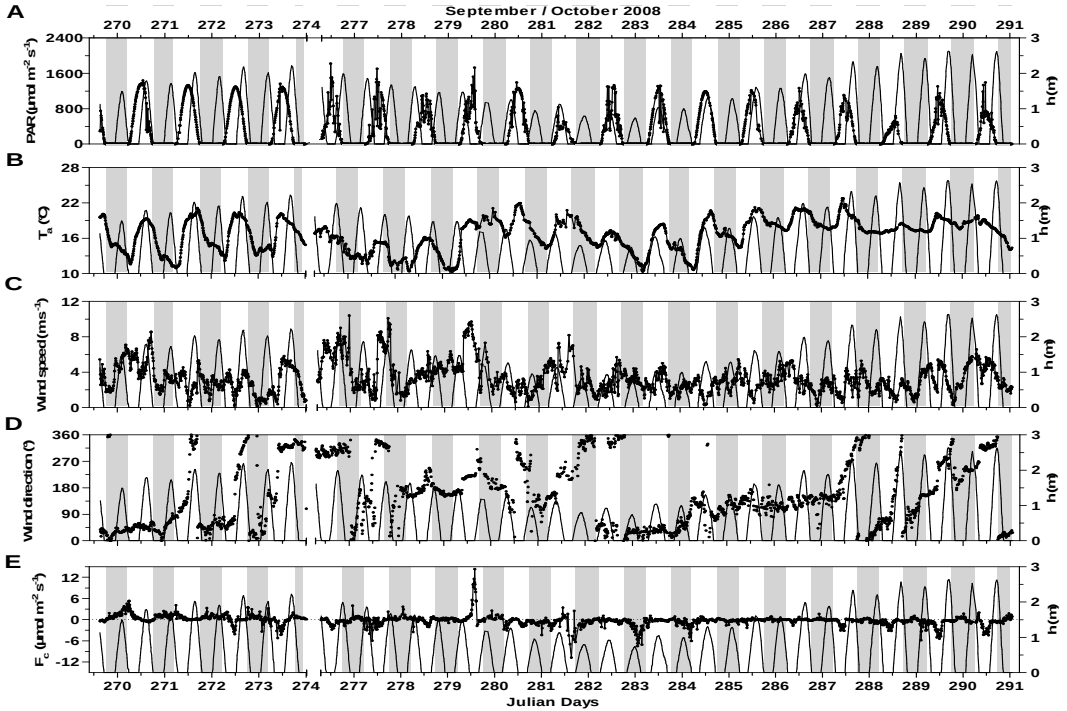

Fig. 5. Environmental parameters and carbon dioxide fluxes measured during the EC deployment in the Arcachon lagoon (St. 1) from 25 September at 15:10 to 17 October 2008 at 01:10 (GMT). **(A)**: photosynthetically active radiation PAR (µmol m^{-2} s^{-1}) and water height (m); **(B)**: temperature of the air (°C); **(C)**: wind speed (m s^{-1}); **(D)**: wind direction (°) and **(E)**: carbon dioxide fluxes (µmol m^{-2} s^{-1}). Negative fluxes represent sinks of CO_2, and positive fluxes represent sources of CO_2 to the atmosphere by convention. Day 269 squares with 25 September 2008, and grey bands represent night periods. Data between 30 September (00:10) and 2 October 2008 (07:10) could not be measured due to technical problems during the deployment. A PAR threshold of 20 µmol m^{-2} s^{-1} was chosen to separate day and night cases, and low tide cases correspond to zero-water heights. A specific range for F_c (panel **E**) was chosen for a better visualisation of CO_2 flux variations.

BGD
8, 5451–5503, 2011

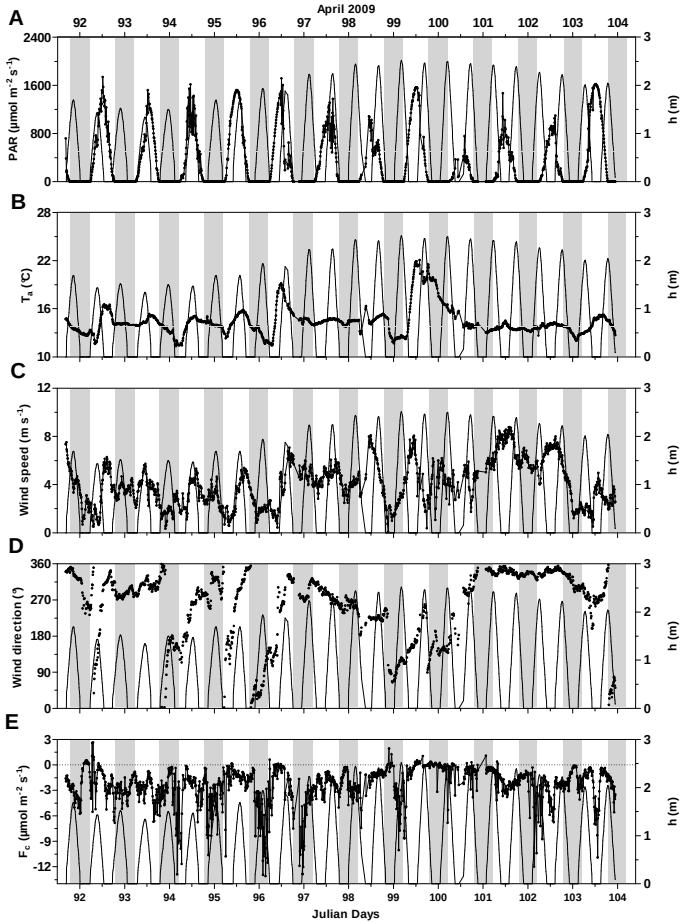

Fig. 6. (Caption on next page.)

BGD
8, 5451–5503, 2011

Fig. 6. Environmental parameters and carbon dioxide fluxes measured during the EC deployment in the Arcachon lagoon (St. 1) from 1 April at 16:30 to 13 April 2009 at 22:50 (GMT). **(A)**: photosynthetically active radiation PAR ($\mu mol\,m^{-2}\,s^{-1}$) and water height (m); **(B)**: temperature of the air (°C); **(C)**: wind speed ($m\,s^{-1}$); **(D)**: wind direction (°) and **(E)**: carbon dioxide fluxes ($\mu mol\,m^{-2}\,s^{-1}$). Negative fluxes represent sinks of CO_2, and positive fluxes represent sources of $CO_2$to the atmosphere by convention. Day 91 squares with 1 April 2009 and grey bands represent night periods. A PAR threshold of $20\,\mu mol\,m^{-2}\,s^{-1}$ was chosen to separate day and night cases, and low tide cases correspond to zero-water heights. A specific range for F_c (panel **E**) was chosen for a better visualisation of CO_2 flux variations.

BGD
8, 5451–5503, 2011

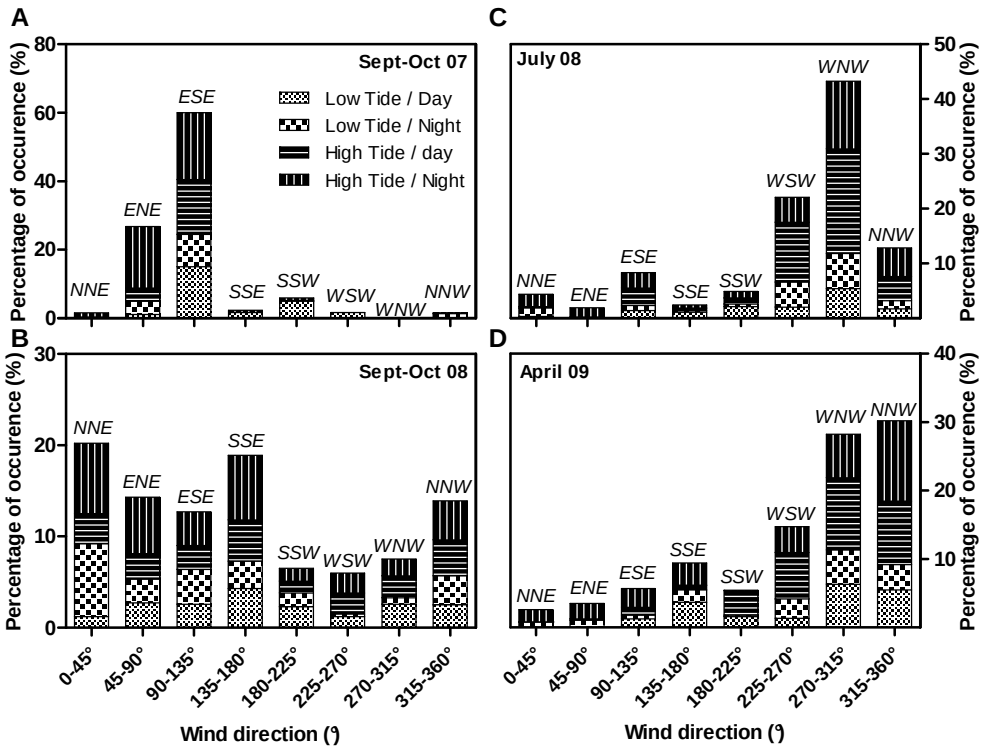

Fig. 7. The wind directions during the four EC measurements in the Arcachon lagoon by percentage of occurrence and functions to the tidal and diurnal rhythms (low tide/day, low tide/night, high tide/day and high tide/night). **(A)**: 30 September to 3 October 2007 (St. 2), **(B)**: 25 September to 17 October 2008 (St. 1), **(C)**: 1 to 7 July 2008 (St. 1) and **(D)**: 1 to 13 April 2009 (St. 1). NNE: north-northeast; ENE: east-northeast, ESE: east-southeast, SSE: south-southeast; SSW: south-southwest; WSW: west-southwest; WNW: west-northwest and NNW: north-northwest wind directions.

BGD
8, 5451–5503, 2011

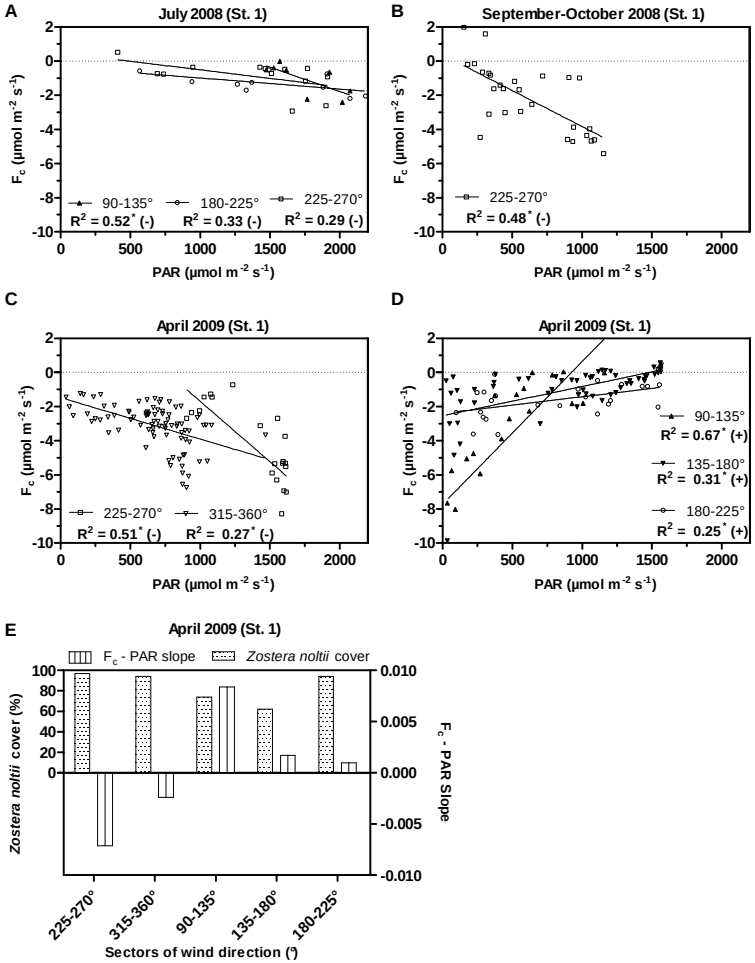

Fig. 8. (Caption on next page.)

BGD
8, 5451–5503, 2011

Fig. 8. P/I linear regressions obtained at low tide during the day in the Arcachon lagoon according to wind directions; **(A)**: July 2008 (Station 1); $-0.003x + 3.91$ (90–135°); $-0.0006x - 0.34$ (180–225°); $-0.001x + 0.50$ (225–270°). **(B)**: September–October 2008 (Station 1); $-0.004x + 0.38$ (225–270°). **(C)** and **(D)**: April 2009 (Station 1); $-0.007x + 5.40$ (225–270°); $-0.002x - 1.47$ (315–360°); $0.008x - 7.73$ (90–135°); $0.002x - 2.54$ (135–180°); $0.001x - 2.40$ (180–225°). **(E)**: F_c-PAR slopes (**C** and **D**) versus *Zostera noltii* covers in April 2009. F_c: Carbon dioxide fluxes; PAR: photosynthetically active radiation; 0–45°: north-northeast; 45–90°: east-northeast, 90–135°: east-southeast, 135–180°: south-southeast, 180–225°: south-southwest; 225–270°: west-southwest; 270–315°: west-northwest and 315–360°: north-northwest wind directions. Notice that F_c values obtained in July 2008 corresponding to PAR values above 2200 µmol m^{-2} s^{-1} have not been taken into account for correlations, these PAR values correspond to non-realistic data due to quantum sensor noise. Additionally, F_c values obtained in July 2008 during the beginning of the experiment (days 183, 184) and in September–October 2008 (day 279) have been discarded representing destocking but not biological degassing by respiration (Figs. 5f and 6f). PAR data in September–October 2007 have been transformed in µmol m^{-2} s^{-1} from global radiation data in W m^{-2} assuming a factor 2 from global radiation to PAR values. * denotes the significance of the linear regressions (p-values below 0.05).

BGD
8, 5451–5503, 2011

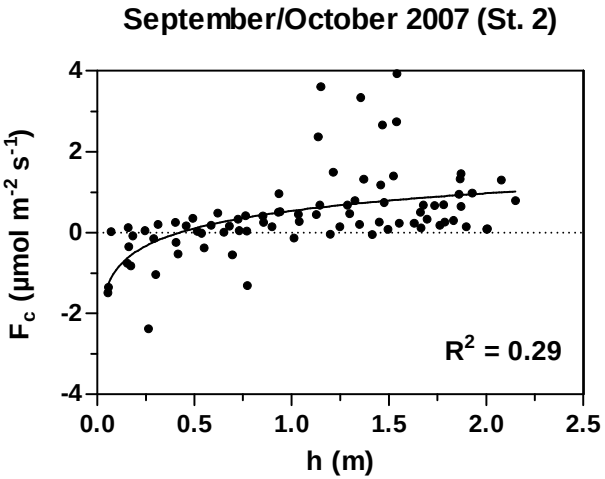

Fig. 9. Carbon dioxide fluxes (F_c) in September–October 2007 (St. 2) during immersion as a function of the water height (h). Beyond 50 cm, the lagoon changed from a sink of CO_2 into a source of CO_2 to the atmosphere.

BGD
8, 5451–5503, 2011